Towards Structural and Functional Investigation of the Nisin Transporter

Gyana Prakash Mahapatra

Department of Anatomy and Cell Biology

McGill University

Montreal, Quebec, Canada

H3A 0B8

March 2023

A thesis submitted to McGill University in partial fulfillment of the requirements of the degree of Master of Science

Table of Contents

Abstract:

Many human pharmaceuticals are derived from natural products and their semi-synthetic analogs. The ribosomally synthesized and post-translationally modified peptides, known as Lanthipeptides, are a structurally diverse class of natural products with potent antimicrobial activities. One of the most extensively studied lanthipeptides is Nisin, produced by the Gram-positive bacterium *Lactococcus lactis* that have attracted considerable interest as an alternative or adjunct to existing antibiotics. Like all lanthipeptides, Nisin possesses thioether linkages that are critical for its biological activity. These thioether linkages are formed in a multistep enzymatic pathway involving dehydration of serine/threonine residues in precursor peptide (NisA), followed by intramolecular addition of cysteine thiols onto the nascent dehydration sites to form (methyl)lanthionine macrocycles. The dehydration and cyclization reactions are governed by the enzymes NisB and NisC, respectively. The NisT ATP-binding cassette (ABC) transporter is then required for the secretion of modified NisA across the bacterial membrane, which is then proteolyzed by NisP to yield mature Nisin. The ABC transporter NisT plays an important role in the biosynthesis of Nisin. NisT is unique since it is specific to the transport of the NisA precursor peptide and is not found in other organisms. This export mechanism is important for the activity of lanthipeptides as an antimicrobial agent, where it exerts its effect on neighboring bacteria. Therefore, a detailed understanding of the substrate recognition and translocation mechanism of the ABC transporter NisT, would be beneficial for engineering and synthetic biology applications. Additionally, understanding how NisT recognizes and transports its substrate, the modified NisA precursor peptide, could be used in the development of biosensors or biosynthetic pathways for the production of other analogous or modified natural products.

Here, we have shown the extensive optimization of NisT purification by screening a wide range of detergents. Following our successful NisT purification, we analyzed and confirmed its ATPase activity in the absence of its substrate (NisA). We also visualized purified NisT by negative staining using Transmission electron microscopy (TEM) and discussed our efforts toward determining the high-resolution structure determination of NisT using cryo-electron microscopy (cryo-EM). Lastly, we present results from the initial experimental setup of Hydrogen–Deuterium Exchange Mass Spectrometry (HDX-MS), which could help us understand the conformational dynamics of NisT.

Résumé:

De nombreux produits pharmaceutiques humains sont dérivés de produits naturels et de leurs analogues semi-synthétiques. Les peptides synthétisés par le ribosome et modifiés après la traduction, connus sous le nom de Lanthipeptides, constituent une classe structurellement diversifiée de produits naturels dotés de puissantes activités antimicrobiennes. L'un des lanthipeptides les plus étudiés est la nisine, produite par la bactérie Gram-positive Lactococcus lactis qui a suscité un intérêt considérable en tant qu'alternative ou complément aux antibiotiques existants. Comme tous les lanthipeptides, la nisine possède des liaisons thioéther essentielles à son activité biologique. Ces liaisons thioéther sont formées dans une voie enzymatique en plusieurs étapes impliquant la déshydratation des résidus sérine/thréonine dans le peptide précurseur (NisA), suivie de l'addition intramoléculaire de thiols de cystéine sur les sites de déshydratation naissants pour former des macrocycles de (méthyl) lantionine. Les réactions de déshydratation et de cyclisation sont régies respectivement par les enzymes NisB et NisC. Le transporteur NisT ATP-binding cassette (ABC) est alors requis pour la sécrétion de NisA modifié à travers la membrane bactérienne, qui est ensuite protéolysée par NisP pour donner de la nisine mature. Le transporteur ABC NisT joue un rôle important dans la biosynthèse de la nisine. NisT est unique car il est spécifique au transport du peptide précurseur NisA et ne se trouve pas dans d'autres organismes. Ce mécanisme d'exportation est important pour l'activité des lanthipeptides en tant qu'agent antimicrobien, où il exerce son effet sur les bactéries voisines. Par conséquent, une compréhension détaillée du mécanisme de reconnaissance du substrat et de translocation du transporteur ABC NisT serait bénéfique pour les applications d'ingénierie et de biologie synthétique. De plus, comprendre comment NisT reconnaît et transporte son substrat, le peptide précurseur NisA modifié, pourrait être utilisé

dans le développement de biocapteurs ou de voies de biosynthèse pour la production d'autres produits naturels analogues ou modifiés.

Ici, nous avons montré l'optimisation poussée de la purification NisT en criblant une large gamme de détergents. Suite à notre purification NisT réussie, nous avons analysé et confirmé son activité ATPase en l'absence de son substrat (NisA). Nous avons également visualisé NisT purifié par coloration négative à l'aide de la microscopie électronique à transmission (TEM) et discuté de nos efforts pour déterminer la détermination de la structure à haute résolution de NisT à l'aide de la cryo-microscopie électronique (cryo-EM). Enfin, nous présentons les résultats de la configuration expérimentale initiale de la spectrométrie de masse par échange hydrogène-deutérium (HDX-MS), qui pourraient nous aider à comprendre la dynamique conformationnelle de NisT.

Acknowledgements:

I have great pleasure in expressing my sincere thanks to everyone who has contributed to the successful completion of my research work. First and foremost, I would like to express my heartfelt gratitude to my supervisor, Dr. Natalie Zeytuni, for providing me with invaluable and consistent guidance throughout my research journey. I am deeply grateful for the scientific freedom, constant encouragement, valuable comments, and fruitful discussions that she provided at every stage of my work.

I would also like to extend my sincere thanks to my committee members for their scientific suggestions, which helped me to shape my research in a meaningful way. My collaborators, Dr. Christopher J. Thibodeaux and Nuwani Weerasinghe deserve a special mention for their valuable contributions to my research. Their expertise and knowledge have been instrumental in advancing my research, and I am grateful for their collaboration.

I would also like to express my sincere gratitude to FEMR and McGill University for providing us with funding and infrastructure support, which has been instrumental in making this research possible. I am grateful for their continued support and dedication to advancing scientific research.

I would like to express my special thanks to my lab mates for their immense support and guidance, which made my research work enjoyable and rewarding. I am also grateful to my friends for their unwavering support, which has been a constant source of motivation and encouragement for me.

Lastly, I owe my deepest gratitude to my dear parents, who have been a constant source of love, encouragement, and support throughout my life. I am immensely grateful for their unwavering belief in me and for always being there for me. Their support has been instrumental in my academic success, and I will always be indebted to them.

List of Figures

List of Tables

Abbreviations

AMR	Antimicrobial resistance
ABC	Adenosine 5′-triphosphate Binding Cassette
MFS	Major Facilitator Superfamily
MATE	Multidrug and Toxin Extrusion
SMR	Small Multidrug Resistance
RND	Resistance-Nodulation-cell Division
PACE	Proteobacterial Antimicrobial Compound Efflux
ATP	Adenosine 5′-triphosphate
VISA	Vancomycin-intermediate resistance *Staphylococcus aureus*
hVISA	Hetero-resistant vancomycin-intermediate *Staphylococcus aureus*
CAT	Chloramphenicol acetyltransferase
HTS	High-Throughput Screening
Cryo-EM	Cryo-electron microscopy
NMR	Nuclear Magnetic Resonance
NRPS	Non-ribosomal peptide synthetase
RiPPs	Ribosomally synthesized and Post-translationally modified Peptides
PTM	Post-translational modification
TMD	TransMembrane Domain
NBD	Nucleotide-Binding Domain
SBP	Substrate-binding protein
P-gp	P-glycoprotein
MRP	Multidrug resistance protein
TMH	Transmembrane helices
NisT	Nisin transporter
Dha	Dehydroalanine
Dhb	Dehydrobutyrine
L. lactis	*Lactococcus lactis*
µg	Microgram
µl	Microlitre
µM	MicroMolar
ml	Millilitre

°	Degrees
OD	Optical density
KCL	Potassium chloride
β-ME	β-mercaptoethanol
mM	MiliMolar
hr	Hour
$MgSO_4$	Magnesium sulfate
HCl	Hydrochloric acid
NaCl	Sodium chloride
w/v	Weight per volume
FC-16	Fos-Choline-16
DDM	Dodecyl-B-D-Maltoside
UDM	n-Undecyl-Beta-Maltoside
LMNG	Lauryl Maltose Neopentyl Glycol
CYMAL-7	Cyclohexyl-Methyl-β-D-Maltoside
LDAO	N, N-Dimethyl-n-dodecylamine N-oxide
kDa	Kilo Dalton
SEC	Size exclusion column
SDS-PAGE	Sodium dodecyl-sulphate polyacrylamide gel electrophoresis
CN-PAGE	Clear native polyacrylamide gel electrophoresis
NSPr	Nanodisc scaffold protein reversed
CMC	Critical micelle concentration
ADP	Adenosine diphosphate
ATP	Adenosine triphosphate
AMP-PNP	Adenylyl-imidodiphosphate
EM	Electron microscopy
ATPγS	Adenosine 5'-O-(3-thiotriphosphate)
HDX-MS	Hydrogen–deuterium exchange mass spectrometry
LC-MS	Liquid chromatography–mass spectrometry
CTF	Contrast Transfer Function

Contribution of Authors

All work done in this thesis was conducted solely by the author except the HDX-MS data collection, which was done by Nuwani Weerasinghe from Dr. Christopher J. Thibodeaux's lab, Department of Chemistry, McGill University.

1. Introduction:

A large number of human pharmaceuticals are derived from natural products and their semi-synthetic analogs. The ribosomally synthesized and post-translationally modified peptides (RiPPs), also known as Lanthipeptides, are a structurally diverse class of natural products with potent antimicrobial, antiviral, and other activities[2]. Importantly, RiPPs possess characteristics that render them promising targets for the engineering of novel drugs. Namely, *all RiPPs are genetically encoded*, providing access to large libraries of variants for cell-based screening and functional engineering[3]. Secondly, most RiPPs are post-translationally modified by *biosynthetic enzymes with relaxed substrate specificity* – a property that is essential for successful engineering[4].

One of the most extensively studied lanthipeptides is Nisin, produced by the Gram-positive bacterium *Lactococcus lactis*. Nisin has been commonly used in the food industry for over 40 years without any substantial development of bacterial resistance. Like all lanthipeptides, Nisin possesses thioether linkages that are critical for its biological activity. These thioether linkages are formed in a multistep enzymatic pathway involving dehydration of serine/threonine residues in the genetically encoded Nisin precursor peptide (NisA), followed by intramolecular addition of cysteine thiols onto the nascent dehydration sites to form (methyl)lanthionine macrocycles[5]. The dehydration and cyclization reactions are governed by the enzymes NisB and NisC, respectively. The modified NisA (mNisA) is then exported across the bacterial membrane by the exporter protein NisT, and then proteolyzed by NisP to yield mature Nisin[5].

NisT transporter is an essential part of the nisin biosynthesis pathway, and its proper function is crucial for the production of the active form of nisin[6]. The exporter protein NisT, belongs to the superfamily of ABC transporters, which is composed of mainly two domains: a

transmembrane domain (TMD) important for substrate translocation and a nucleotide-binding domain (NBD), which binds and hydrolyses ATP to energize conformational changes used for substrate translocation. During the substrate translocation cycle, ABC transporters undergo significant conformational changes between inward open, occluded, and outward open states. The NisT transporter is required for the secretion of NisA and uses the leader peptide for substrate recognition.

1.1 Rational and Objectives of the Thesis:

A detailed understanding of the substrate recognition and translocation mechanism of the ABC transporter NisT, would be beneficial for engineering and synthetic biology applications. For example, in the biotechnology field, an understanding of the substrate recognition and translocation mechanism of NisT could be used to optimize the production of nisin or to engineer new antimicrobial peptides with improved properties. In the field of synthetic biology, knowledge of the NisT mechanism could be used to engineer bacteria with improved secretion systems, allowing them to produce and secrete a wider variety of peptides and other bioactive molecules.

By understanding the secretion mechanism of NisT, researchers could potentially design similar transporters for use in other organisms, such as yeast or *E. coli*, to improve modified peptide secretion and production for industrial or therapeutic applications. Additionally, the obtained knowledge of how NisT recognizes and transports its substrate, the modified NisA precursor peptide, could also be used in the development of biosensors or biosynthetic pathways for the production of other natural products.

My thesis's overall aim is the structural and functional characterization of the Nisin transporters NisT in *L. lactis*. My specific objectives are:

1. High-resolution structure determination of NisT in different states.
2. Mechanistic and enzymatic characterization of the NisT exporter.

2. A comprehensive review of the literature:

2.1 The Emergence and Mechanism of Antimicrobial Resistance:

Antimicrobial resistance (AMR) has emerged as one of the biggest threats to global health and is recognized as a major concern in the treatment of microbial infections[7]. AMR refers to the ability of microorganisms such as bacteria, viruses, fungi, and parasites to resist the effects of antimicrobial drugs, such as antibiotics, antivirals, and antifungals. This resistance can occur naturally or due to the overuse or misuse of antimicrobial drugs. As a result, the drugs become futile and infections persist in the body, increasing the risk of spreading to other people. Alongside devastating viral pandemics such as SARS-CoV-2, the rise of antibiotic-resistant bacterial pathogens represents an immense threat to human health and the world economy[8]. According to a recent study, 1.27 million deaths were estimated globally due to antimicrobial-resistant bacterial infections in 2019 alone[9]. Furthermore, as the development of resistance towards existing antibiotics exceeds the development of new therapies, multiple resistant infections are predicted to be the leading cause of death by 2050, even surpassing cancer[10,11]. Nowadays, the treatment options for infections caused by antimicrobial-resistant bacteria are limited and most drugs in the pharmaceutical development pipeline are modifications of existing classes of antibiotics[12].

The emergence of AMR is a complex process influenced by various factors, including genetic mutations, the spread of resistant strains of microorganisms, and the overuse of antimicrobial drugs in both human and animal populations[13]. One of the main mechanisms of antimicrobial resistance is the presence of specific genes, which encode for proteins that confer resistance to antibiotics and other antimicrobial agents[14]. These proteins can directly alter the target of the antimicrobial drug, inactivate the drug, pump the drug out of the bacterial cell, or alter metabolic pathways to prevent the drug from having an effect[15]. These genetically encoded resistance mechanisms provide the bacteria with a survival advantage, allowing them

to continue and replicate even when in the presence of the antimicrobials that would typically kill or inhibit them. These resistance genes can be transferred between microorganisms through mechanisms such as horizontal gene transfer, which allows the rapid spread of resistance among different species of microorganisms. Other resistance mechanisms include efflux pumps to remove any toxic antimicrobials, inactivation of a drug where the chemical structure of the drug is altered - rendering it inactive or less effective, and finally, mutation in the target site of the antimicrobial, making it difficult for the drug to bind to the microorganism.

Overall, bacteria have evolved with three main sophisticated mechanisms of resistance to survive in the presence of specific antimicrobial molecules[16]. Each of these mechanisms is described in the following sections.

2.1.1 Efflux pumps:

Efflux pumps are chromosomally or plasmid-encoded genes, that play a vital role in AMR[17]. These pumps are commonly found in the cell membrane of Gram-positive and Gram-negative bacteria[18]. Efflux pumps are transport proteins that recognize and pump toxic substances, such as antibiotics, out of the cell and serve as an intrinsic mechanism to protect bacteria in a hostile environment. Among the different resistant mechanisms, efflux pumps are the fastest-acting and most effective resistance mechanism in the bacteria[19]. Six families of bacterial drug efflux pump that contribute to the efflux pathways have been identified. These efflux pumps families include the Adenosine 5′-triphosphate Binding Cassette (ABC) family, Major Facilitator Superfamily (MFS), Multidrug and Toxin Extrusion (MATE) family, Small Multidrug Resistance (SMR) family, Resistance-Nodulation-cell Division (RND) superfamily and Proteobacterial Antimicrobial Compound Efflux (PACE) family[20]. These pumps either use Adenosine 5′-triphosphate (ATP), the cell's energy currency, or proton gradients to drive the transport process of the antimicrobial outside of the cell[21]. Some efflux pumps present a specificity to certain classes of drugs, while others pump out a wide range of drugs[22]. Efflux

pumps can confer resistance to multiple classes of drugs, including antibiotics, antivirals, and antifungals, making the microorganisms resistant to multiple drugs at once. This mechanism is known as multidrug resistance, which makes treating infections caused by these microorganisms even more challenging.

2.1.2 Modification of a drug target:

The modification of a drug target refers to the process of the alteration of target proteins, enzymes, or other molecules, making them less susceptible to the antimicrobial. Modifying drug targets is a complex process that can occur naturally or following a drug exposure[23]. The process can also be mediated by resistance genes that encode for additional enzymes or proteins that can modify the target site of drugs, making it more difficult for drugs to bind and exert their effect[23]. Moreover, some bacteria have developed mechanisms to modify their cell wall, making them less susceptible to the action of antibiotics, such as vancomycin[16]. For example, vancomycin conferred resistance includes the alteration of the vancomycin binding site at the C-terminal of the D-Ala-D-Ala residues peptidoglycan precursor [24]. This alteration can be achieved by mutation in the genes that encode for the enzymes involved in peptidoglycan synthesis. Additional mechanism is the production of modified peptidoglycan precursors such as D-Ala-D-Lactate, which vancomycin cannot recognize as a target. This type of resistance is known as vancomycin-intermediate resistance (VISA) or hetero-resistant vancomycin-intermediate *Staphylococcus aureus* (hVISA)[25]. Another example includes the modification of the target binding site of a drug, such as a mutation in the bacterial ribosome, a common mechanism that is conferred by antibiotics such as tetracyclines and macrolides[16]. Ribosome mutation can also lead to the formation of a new binding/catalytic site to which the drug cannot bind, thus, making the bacteria resistant to the drug[26].

2.1.3 Inactivation of a drug:

Inactivation of a drug by bacteria is a process that occurs when bacteria break down or alter the chemical structure of a drug, making it less effective. This drug inactivation occurs through various mechanisms, including metabolism by bacterial enzymes or the production of enzymes that inactivate drugs[27]. For example, chloramphenicol is a broad-spectrum antibiotic that is effective against a wide range of bacteria, including those that cause meningitis, sepsis, and typhoid fever[28]. The mechanism of chloramphenicol resistance in bacteria occurs through the production of chloramphenicol acetyltransferase (CAT)[29], which can irreversibly inactivate chloramphenicol by acetylating the antibiotic, preventing it from binding to the bacterial ribosome and, and thus, inhibit protein synthesis. Another example includes the modification of bacterial enzymes, such as the beta-lactamases family. Beta-lactamases are responsible for the chemical breakdown of beta-lactam antibiotics such as penicillin and cephalosporins[30]. Bacteria can produce a wide range of beta-lactamases, some of which can hydrolyze a broad range of beta-lactam antibiotics[31]. Other bacteria can also produce aminoglycoside acetyltransferases, which can inactivate aminoglycoside antibiotics such as streptomycin, and neomycin[32].

2.2 The traditional process of drug discovery:

The problem of antimicrobial resistance has challenged the traditional drug discovery process over the recent decades. During the conventional drug discovery pipeline, lead drug candidates are optimized for efficacy and safety, and the most promising candidates are then tested in clinical trials[33]. However, the prolonged duration of this process, combined with the ability of microorganisms to rapidly develop new resistance to new drugs, has made it difficult to develop new drugs that are effective against antimicrobial-resistant infections by the time they are deemed safe to use[34]. These traditional approaches are still widely used but have limitations,

including high costs and the potential for false-positive results[34]. As a result, there is a growing interest in developing new approaches for drug discovery that are more efficient and effective.

2.3 Modern approaches for drug discovery:

As bacteria continue to develop resistance to new and existing drugs, it becomes more difficult to treat infections and increases the risk of treatment failure[14]. The current situation calls for the development of new drugs to substitute or supplement the existing antimicrobials repository. However, the development of new drugs, including antibiotics, is a complex and expensive process that can take years and involves multiple stages of research and development, clinical trials, and regulatory approvals. In recent years, there has been a decline in the number of new antibiotics being approved, partly due to the challenges and costs associated with developing new drugs, as well as regulatory hurdles and the emergence of antibiotic-resistant bacteria[35]. As a result, the drug discovery and development pipeline has undergone several changes to include new platforms to increase efficiency. The next section will provide a description of these platforms.

2.3.1 High-Throughput Screening (HTS):

HTS is a method that uses automated equipment to screen through large numbers of chemical compounds activity against a biological target of interest. The screened compounds can be small molecules or biomolecules such as peptides, nucleic acids, or antibodies[36]. The biological targets include enzymes, receptors, or other proteins involved in disease manifestation. HTS can also screen for various activities, including enzyme inhibition, receptor binding, or gene expression modulation[37]. One of the main advantages of HTS is its speed and efficiency. HTS allows for the rapid screening of large numbers of compounds, which increases the likelihood of identifying new drug candidates. Additionally, HTS allows for the screening of diverse chemical libraries, which increases the probability of identifying new chemical scaffolds that

can be developed into drugs[38]. However, HTS also has some limitations. One limitation is that it typically only identifies compounds with moderate to strong activity against the target. Hence, HST might fail to identify compounds with a weak activity that could be further optimized to become drugs. Additionally, HTS does not provide information about the pharmacokinetics, pharmacodynamics and toxicity of the compounds, which are important aspects of drug development[39].

2.3.2 Computational drug discovery:

The computational drug discovery approach involves using computer-aided methods to predict the potential activity of compounds and design new molecules. This approach is becoming a crucial part of the recent drug discovery as it allows for the rapid and efficient exploration of large numbers of chemical compounds, while predicting their potential activity[40]. Several techniques are commonly used hand in hand during computational drug discovery, including:

(i) Molecular modelling: Computer simulations to predict the three-dimensional structure of molecules and their interactions with biological targets.

(ii) Virtual screening: Computational methods to search large libraries of chemical compounds for those that are likely to bind to a specific target.

(iii) Computational chemistry: Computational methods to predict the properties of chemical compounds, such as solubility, stability, and toxicity.

(iv) Machine learning and artificial intelligence: These methods are used to analyze large datasets and to identify patterns in the data that can be used to predict the activity of compounds.

Since this platform is based on computational models and simulations, the models produced by these predictions might not always be accurate. Additionally, computational methods can only predict the activity of compounds *in silico*, and therefore, it is crucial to continue and validate these predictions experimentally.

2.3.3 Target-based drug discovery:

Target-based drug discovery method involves identifying specific targets in the host system, such as enzymes or receptors, that are involved in a disease or physiological process, and then designing drugs that interact with and modulate those targets to achieve a desired therapeutic effect[23]. The target-based drug discovery process begins with the identification of a target protein followed by its three-dimensional structure determination by techniques such as, cryo-electron microscopy (cryo-EM), X-ray crystallography, or Nuclear Magnetic Resonance (NMR). Once the atomic structure is determined, computational methods can be used to search large libraries of chemical compounds that are likely to bind to the target protein. These compounds can then be tested experimentally to confirm their target binding ability and whether it can modulate its activity[41]. Target-based drug discovery has become an increasingly popular approach, as advances in genomics and proteomics have made it possible to identify and characterize specific molecular targets with greater precision.

2.3.4 Phenotypic screen-based drug discovery:

Phenotypic screen-based drug discovery is an approach that is based on the observation of the overall effects of compounds on cells or organisms[42]. Unlike target-based drug discovery, where the focus is on identifying a specific protein or enzyme target and developing a drug to modulate its activity, phenotypic drug discovery focuses on identifying compounds that have a desired effect on a disease, without necessarily understanding the underlying target or mechanism of action. In phenotypic screen-based approach, the compounds can be tested in cell-based assays, animal models, or even in human clinical trials. The compounds that show a net positive effect are then further characterized to understand the target and mechanism of action[43]. However, phenotypic drug discovery has some limitations. One limitation is that it can be difficult to identify the target and mechanism of action of a compound that has a positive effect. For example, a compound may produce a desired phenotype by interacting with multiple

targets or by modulating a pathway upstream or downstream of the target. Additionally, the target may not be present in the assay system used for screening, or it may be expressed at very low levels or in a modified form. Identifying the target and mechanism of action of a phenotypic hit typically requires additional studies, such as biochemical or genetic studies, to identify interacting proteins or pathways, or target deconvolution approaches such as chemoproteomics or RNA interference[44]. These studies can be time-consuming, expensive, and might not be successful.

Despite these challenges, there are several advantages to phenotypic drug discovery, including the ability to identify compounds with novel mechanisms of action or activity against multiple targets, and the potential to identify drugs that are effective against complex diseases or conditions where the underlying biology may not be well understood.

2.3.5 Natural products:

Natural products have been an important source of new antibiotic discovery. Natural products are produced by microorganisms, such as bacteria and fungi, and have been used for centuries to treat infections[13]. One of the main advantages of natural products for drug discovery is the exceptional diversity in chemical structures and biological activities that have already been employed by nature and can perhaps be mimicked by us. Many natural products have a complex structure that is difficult to synthesize chemically.

Natural products have been such a rich source of antimicrobials throughout history. Many natural products, such as antibiotics and antivirals, have been discovered from microorganisms, which produce these compounds as part of their natural defence mechanisms[45]. Natural products can be divided into several categories based on their chemical structures, such as alkaloids, flavonoids, terpenes, and polyketides, among others[46].

The diversity of natural products is a result of evolutionary processes, where organisms have developed a wide range of chemical compounds to survive and replicate in challenging

environmental conditions. The diversity in producing microorganisms and their environmental niche reflects the great diversity of natural products, particularly in their chemical structures and biological activities. Natural product diversity is also reflected in the wide range of biosynthetic pathways used for their synthesis. Notably, the vast majority of the natural products producing organisms, such as microorganisms and plants, have yet to be thoroughly investigated. Therefore, despite their abundance and diversity, the majority of natural products have yet to be discovered and characterized. In accordance with natural products' diversity, different families of antibiotic compounds with various structures and mechanisms of action can be found.

There are two major biosynthetic pathways in bacteria that are involved in the production of natural products: non-ribosomal peptide synthesis and ribosomal peptide synthesis[47]. The two pathways fundamentally differ in their mechanism and the types of peptides produced. The non-ribosomal peptide synthesis occurs independent of the ribosome and involves the sequential condensation of amino acids by a multi-enzyme complex called non-ribosomal peptide synthetase (NRPS). This pathway can produce a wide variety of peptides, including cyclic peptides, and linear peptides. Notably, the NRPS pathway is responsible for the production of important antibiotics, including vancomycin and daptomycin and other bioactive compounds[48].

Ribosomal peptide synthesis, unlike NRPS, is the conventional peptide synthesis by the ribosome and involves the translation of template mRNA into peptides. The peptides produced by this pathway are called Ribosomally synthesized and Post-translationally modified Peptides (RiPPs), typically cyclic or linear and often used as structural or regulatory molecules within the organism[3]. Although no RiPP-based drugs are currently on the market, they received considerable attention as viable alternatives for NRPS. While NRPS have proven to be effective antibiotics, the increased resistance to this class of drugs has become a major concern.

In contrast, the RiPPs, with their unique biosynthetic pathways and diverse mechanisms of action, cannot be inhibited by the most common multidrug-resistant bacteria in evolution. In addition, the small gene cluster size of RiPPs contributes to their emerging potential in bioengineering and synthetic biology drug discovery applications.

2.4 Ribosomally synthesized and post-translationally modified peptides (RiPPs):

RiPPs are a large class of natural products and are well known for their structural diversity. Following their initial translation by the ribosome, RiPPs continue to be chemically modified by different enzymes. These modifications, such as cyclization, oxidation, methylation, and maturation, leading to the formation of unique peptide structures that often have biological activity. Due to their unique structures and biological activities, RiPPs have been suggested as a promising source of new drugs, agrochemicals, and industrial enzymes. Some examples of well-characterized RiPPs are the group of cyclic peptides called lantipeptides that include nisin, subtilin, and cyclotides[49-51].

A typical RiPP gene cluster encodes for a series of components involved in the synthesis and modification of a specific natural product. These gene clusters usually include genes encoding for the precursor peptide, the enzymes responsible for post-translational modifications, including transporter and protease enzymes, and regulatory elements[52] (Figure 1). The precursor peptide gene encodes for the linear peptide, which serves as the template peptide where the downstream modifications of the RiPP take place. This precursor peptide gene is typically located near the start of the gene cluster and is transcribed and translated into a linear peptide by the bacteria's ribosome. The post-translational modification (PTM) enzymes are responsible for the introduction of specific modifications to the precursor peptide, such as cyclization, oxidation, methylation, and other chemical modifications, including maturation[52]. These PMT enzymes are encoded by the genes around the middle of the gene cluster (Figure 1). Regulatory elements like promoters and terminators are usually located near the end of the

gene cluster and are responsible for the transcription and translation of the precursor peptide and PTMs.

Notably, the PMT enzymes responsible for RiPP modification and maturation are typically multifunctional and can install modifications at multiple points with high specificity within a precursor peptide substrate. These enzymes are usually composed of multiple domains, each responsible for a specific modification, which produces a wide variety of RiPPs with unique structures and functions.

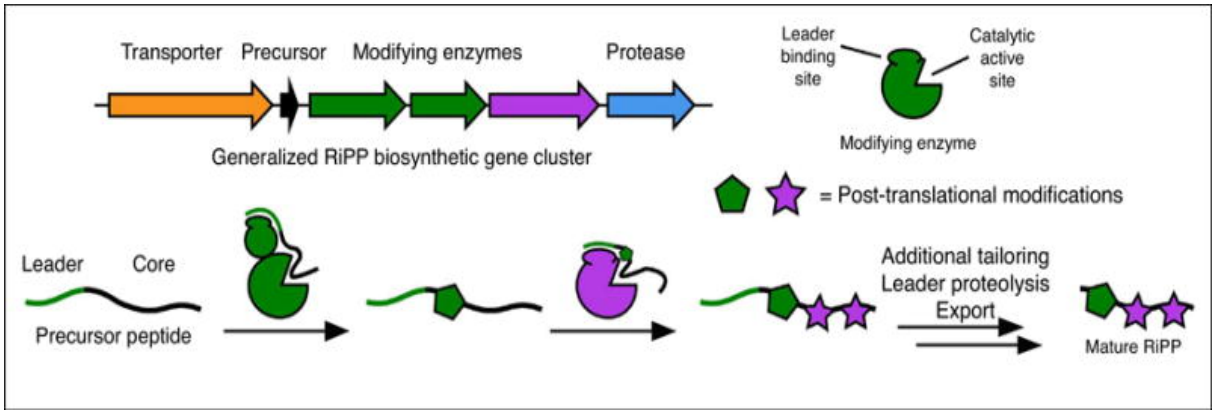

Figure 1. *The biosynthetic pathway of RiPPs adapted from Hudson et al., 2018*[4].

2.5 Lanthipeptides:

The largest and one of the most studied classes of RiPPs are the lanthipeptides. Lanthipeptides are a class of cyclic peptides characterized by the presence of lanthionine or methyllanthionine residues, which are introduced by a specific enzyme called lanthionine synthetase[2]. Lanthipeptides, also called lantibiotics, are known for their wide range of activities, including antibacterial, antifungal, and antiviral activity and have been studied extensively as a source of inspiration for the development of new antibiotics and other bioactive compounds[49].

One of the most extensively studied lanthipeptides is Nisin, produced by the Gram-positive bacterium *Lactococcus lactis*[49]. Nisin can inhibit the growth of a wide range of bacterial genera, including Listeria, Clostridium and Staphylococcus, making it an attractive

candidate for treating infections caused by drug-resistant bacteria as well as food preservation applications[53]. Like all lanthipeptides, Nisin possesses intramolecular thioether linkages (Figure 2). The thioether linkages in Nisin are critical for the biological activity of the compound: the *N*-terminal rings A-C bind to the pyrophosphate moiety of lipid II to inhibit peptidoglycan biosynthesis, while the *C*-terminal D-E rings oligomerize and form pores in the bacterial plasma membrane[54], which eventually disrupts the cell membrane of bacteria and preventing them from growing and multiplying.

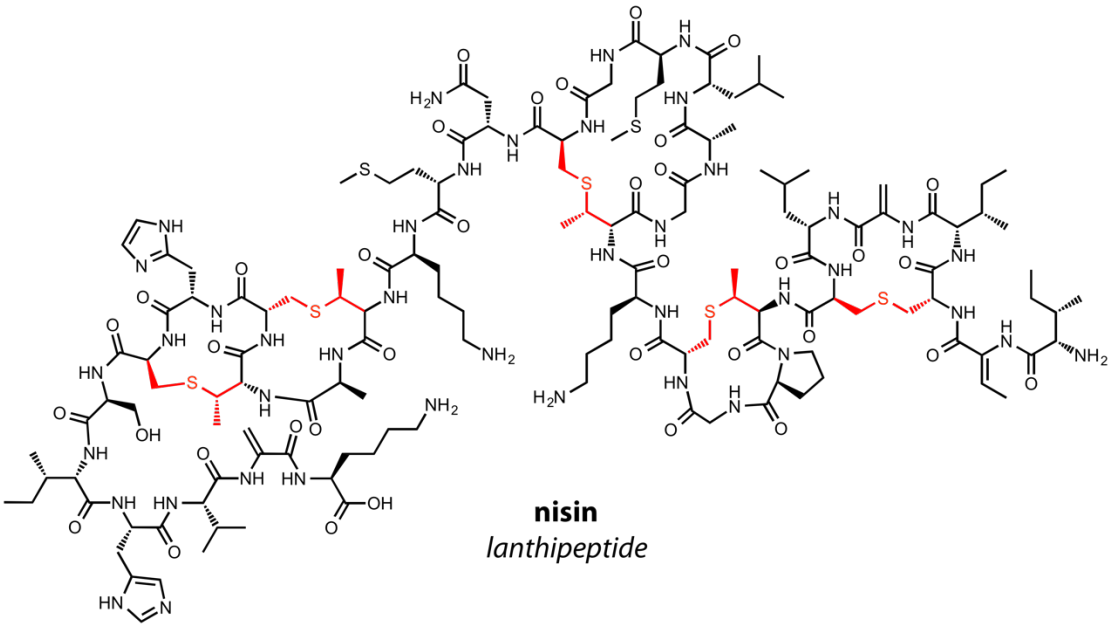

Figure 2. *Chemical structure of Nisin. Adapted from Wikipedia. Thioether rings are coloured red.*

2.5.1 Nisin:

Nisin is produced by the Gram-positive bacterium *Lactococcus lactis* as a precursor peptide known as NisA. All genes responsible for the modification, secretion, and maturation of NisA into the active form of Nisin are located on a single operon (Figure 3A). The nisin biosynthetic operon includes genes that encodes for the enzymes NisB, NisC, NisT, and NisP, which are responsible for the dehydration, cyclization, export and leader peptide cleavage, respectively.

The presence of all the genes on a single operon allows for coordinated regulation of nisin biosynthesis and ensures that the final product is in the optimal form for its intended use[4].

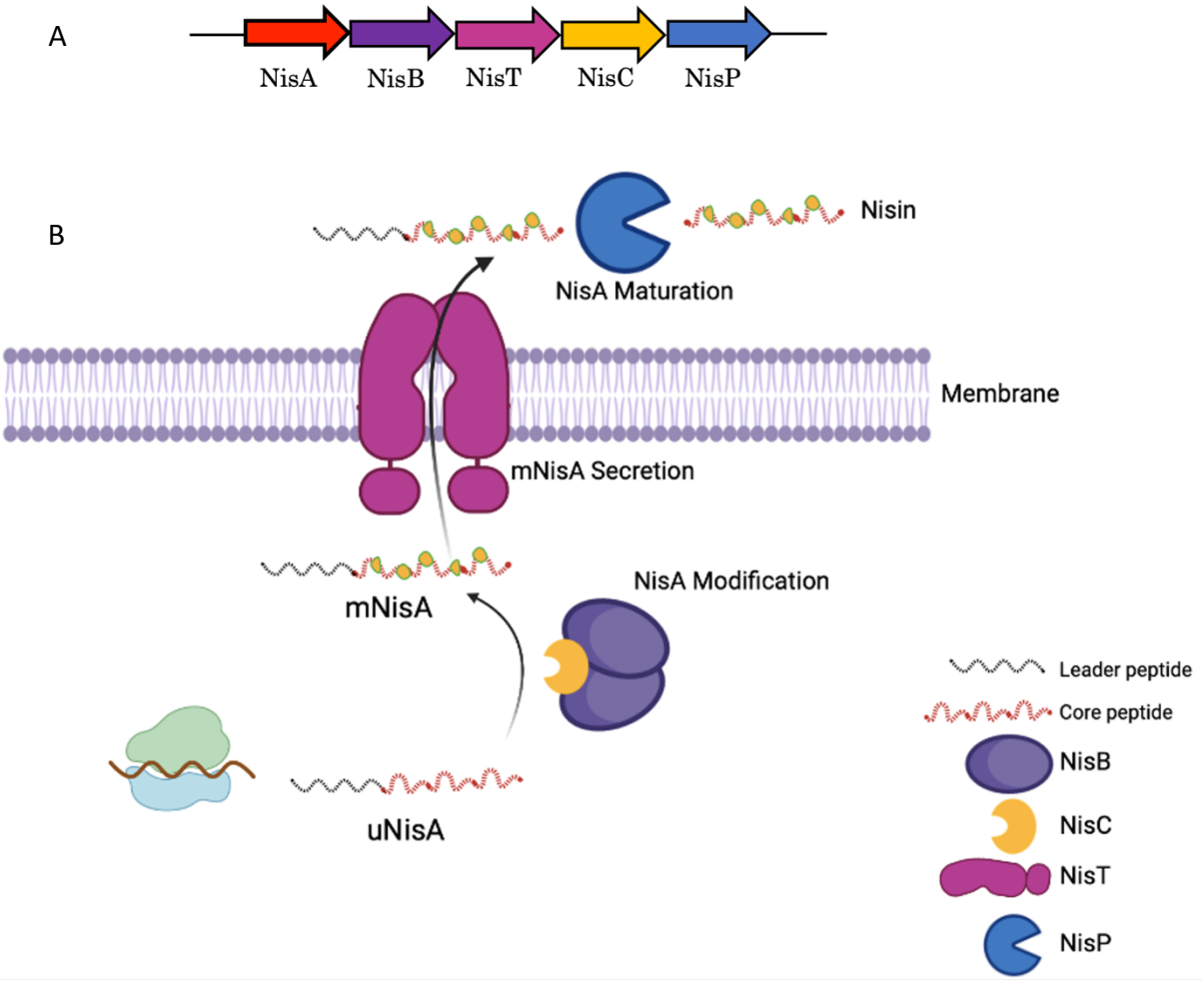

Figure 3. *A) The lanthipeptide Nisin (NisA, red) operon encodes for the modification and secretion enzymes, B) Scheme of Nisin modification and secretion system. Made in BioRender.*

2.5.2. Nisin's precursor peptide modification:

The thioether linkages in Nisin are formed in a multistep reaction pathway involving the dehydration of serine/threonine residues on the NisA precursor peptide, followed by intramolecular addition of cysteine thiols onto the newly formed dehydration sites to form the (methyl)lanthionine macrocycles[2] (Figure 4A). This process is catalyzed by the enzymes NisB and NisC, which perform the dehydration and cyclization reactions, respectively. NisB carries

out the dehydration in a two-step chemical mechanism involving glutamylation of Ser/Thr hydroxyl groups, followed by elimination of the glutamate to make the dehydrated residues (Figure 4B). NisC, on the other hand, uses a zinc ion to lower the pKa of the NisA cysteine thiols and catalyze the formation of the five thioether bridges found in the mature form of nisin[2] (Figure 4B). The catalyzation process is highly precise and specific, with the enzymes showing excellent regio- and stereochemical control over the cyclization reactions. Once the NisA precursor peptide is modified by NisB and NisC, it is exported across the membrane by the NisT transporter. Next, the leader peptide is removed by the NisP protease to produce the active form of nisin. The ATP-binding cassette (ABC) transporter NisT plays an important role in the biosynthesis of Nisin[5]. NisT is unique since it is specific to the transport of the NisA precursor peptide and is not found in other organisms. In a canonical RiPP gene cluster/operon, an ABC transporter translocates the RiPP across the cell's membrane. The nisin export mechanism is important for the entire activity of RiPPs as an antimicrobial agent where it exerts its effect on neighboring bacteria.

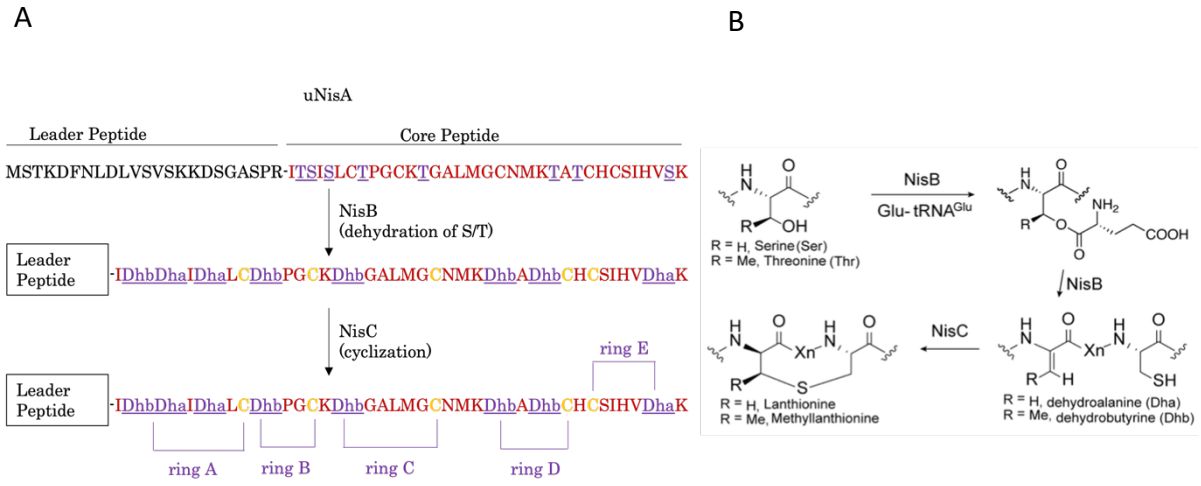

Figure 4. *A) The chemical modifications in Nisin biosynthetic pathway, B) Chemical mechanism of the reactions catalyzed by the NisB dehydratase and the NisC cyclase.*

2.6 ATP-Binding Cassette (ABC) Transporter Overview:

ABC transporters are a large family of transmembrane proteins found in all domains of life. The ABC transporter family was first discovered as a group of transmembrane proteins involved in the uptake of amino acids by bacteria[55]. These proteins were shown to have a common structure consisting of two transmembrane domains and two ATP-binding domains, and therefore called ATP-Binding Cassette transporters. Over time, studies on different bacterial species and other organisms, such as yeast, plants, and animals, have revealed that the ABC transporters family are involved in a wide range of biological processes, including nutrient uptake and bile secretion across the cell membrane[56], detoxification of xenobiotics, and the maintenance of ionic homeostasis[57]. ABC transporters are also responsible for the active transport of a wide range of substrates, including ions, small molecules, and macromolecules, across cellular membranes[1,58]. In humans, ABC transporters are involved in many physiological processes and diseases, including drug resistance, lipid metabolism, and cystic fibrosis[59]. This constitutes ABC transporters as important targets for drug discovery and the development of new therapies for a variety of diseases, including cancer and bacterial infections[60].

2.6.1 General structure:

Canonical ABC transporters fold into two distinct domains: the TransMembrane Domain (TMD) and the Nucleotide-Binding Domain (NBD). Two TMDs are embedded within the lipid bilayer while the two NBDs are facing the cytosol. The NBDs can bind and hydrolyze ATP to provide the energy source for substrate transport and associated conformational changes. The TMD and NBD are

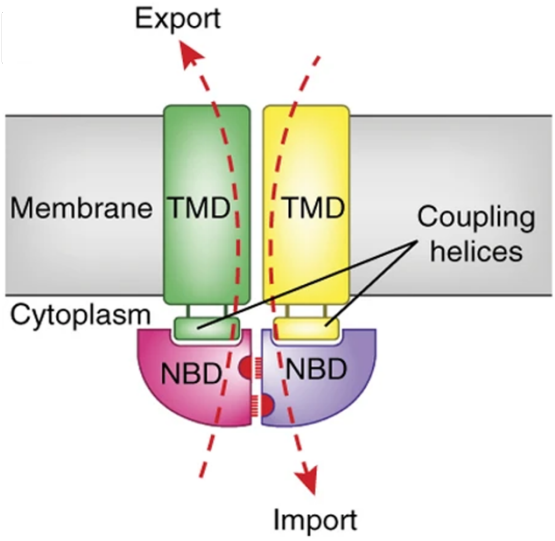

Figure 5. *General structure of an ABC transporter. For every transporter there are two NBDs, two TMDs, and coupling helices at each NBD-TMD junction. Adapted from Rees et al., 2009[1].*

connected by coupling helices (Figure 5), which play a crucial role in linking the conformational changes between the TMDs and NBDs and transmitting the energy derived from ATP hydrolysis to drive substrate transport.

The Nucleotide Binding Domain (NBD):

The NBD of ABC transporters contains several conserved motifs and adopts a conserved fold across the entire ABC transporter family[61]. This high degree of conservation suggests that the NBD plays a critical role in the function of these transporters. Each NBD can be divided into two constituent domains: the RecA domain and the alpha-helical domain[62] (Figure 6 and 7). When these two domains come together, they form two ATP-binding sites, which bind and hydrolyze ATP to provide the energy needed for substrate transport.

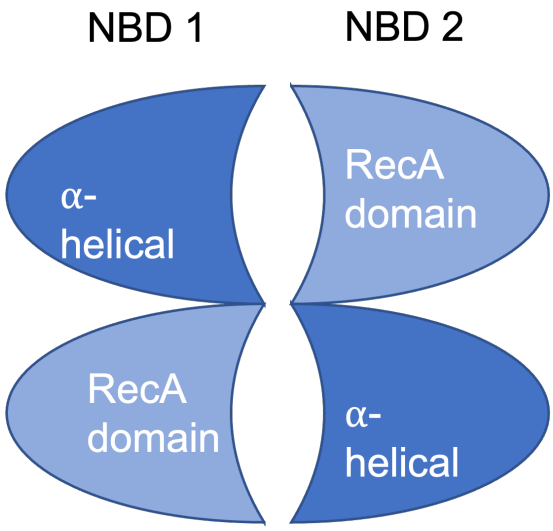

Figure 6. *A simplified structure of the Nucleotide Binding Domain (NBD)*

Two symmetrical ATP-binding sites are formed in the interface between two NBDs. Each site comprises several conserved sequence motifs that are critical for ATP binding and hydrolysis. The Walker A and B motifs, named after the "Walker" consensus sequences, are two highly conserved regions of the ATP-binding site that play key roles in ATP binding and hydrolysis[63]. The Walker A motif, which consists of a lysine residue and a histidine residue, is critical for ATP binding, while the Walker B motif, which consists of a conserved aspartate residue, is essential for ATP hydrolysis[63]. The ABC signature motif is another important component of the ATP-binding site[64], located near the Walker B motif and the ATP-binding site. It is involved in the regulation of ATP hydrolysis, and its specific sequence and structural features are thought to play a role in coordinating ATP binding and hydrolysis with substrate transport.

Together, these motifs form the structural basis of the NBDs, and their specific arrangement and interactions are critical for the efficient and regulated hydrolysis of ATP[65]. By coordinating the binding and hydrolysis of ATP, these motifs play a critical role in the functioning of ABC transporters and other ATP-dependent transporters.

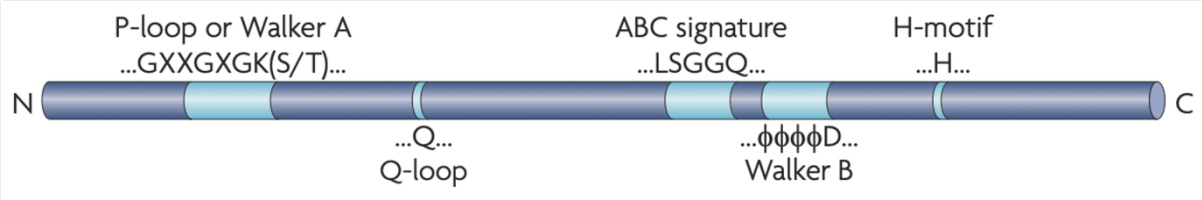

Figure 7. *Location of various conserved regions of the NBD. Adapted from Rees et al., 2009[1].*

The Transmembrane Domain (TMD):

The TMD is a hydrophobic region of the transporter that spans the lipid bilayer of the cellular membrane. It consists of several transmembrane helices, typically ranging from four to six, connected by loops that protrude into the cytoplasm and extracellular space. The TMDs can be arranged as homodimers or heterodimers, forming a substrate-binding pocket that allows the transporter to recognize and bind to its specific substrate. The TMDs are highly selective and can recognize and bind to a diverse range of substrates, including lipids, sugars, ions, and peptides. Each TMD is composed of α-helical segments that span the lipid bilayer. One common feature of TMD is the interaction with NBD via "coupling helices," (Figure 5) which are relatively flexible structures that contain a universal three amino acid motif, EAA (Glu-Ala-Ala)[62]. The coupling helices form non-covalent interactions with the Q-loop of the NBDs and are thus able to respond to structural changes in the NBDs. This interaction between the coupling helices and the Q-loop is crucial for linking the nucleotide state and conformation of the TMDs with that of the NBDs[62]. The coupling helices are also thought to play a key role in transmitting conformational changes between the TMDs and NBDs, linking substrate transport to ATP hydrolysis[65].

2.7 ABC Transporter classification:

ABC transporters can be classified into two main categories based on their substrate transport directionality across the membrane: importers and exporters. The transporters within each group not only share similar structures, but they often share similarities in their mode of action as well, due to the fact that ABC transporters evolved from a common ancestral gene and have diversified over time to perform different functions[66]. Additionally, many ABC transporters within a group like *E. coli* BtuCD[67] and *Archaeoglobus fulgidus* ModBC[68] share conserved sequence motifs and structural features that are critical for their function. These similarities provide important clues to the function and mechanism of these transporters and facilitate the discovery of new transporters and the characterization of their functions.

2.7.1 Importers:

ABC importers, also known as ATP-binding cassette permeases, are responsible for the transport of substrates into the cell, typically against their concentration gradient. ABC importers typically transport small molecules such as ions, sugars, and amino acids, and they are widespread in prokaryotic and eukaryotic organisms[69]. The transport mechanism of importers begins with the binding of the substrate to the periplasmic substrate-binding protein (SBP). The SBP has a high affinity for the substrate and ensures that only the desired molecule is transported. The binding of the substrate induces a conformational change in the SBP, which allows it to interact with the transmembrane domain (TMD) of the transporter[70]. The binding of the substrate to the TMD induces a conformational change that triggers the NBD domain to hydrolyze ATP. The hydrolysis of ATP provides the energy required for substrate translocation across the membrane[71]. The conformational change in the TMD causes the substrate-binding pocket to switch from an inward-facing to an outward-facing state, allowing the substrate to be released on the opposite side of the membrane. The ATP hydrolysis also resets the transporter to its initial state, ready for the next cycle of transport[72]. ABC importers can be classified into

two major categories, such as Type-I and Type-II ABC importers based on their architecture and mechanism of transport (Figure 8).

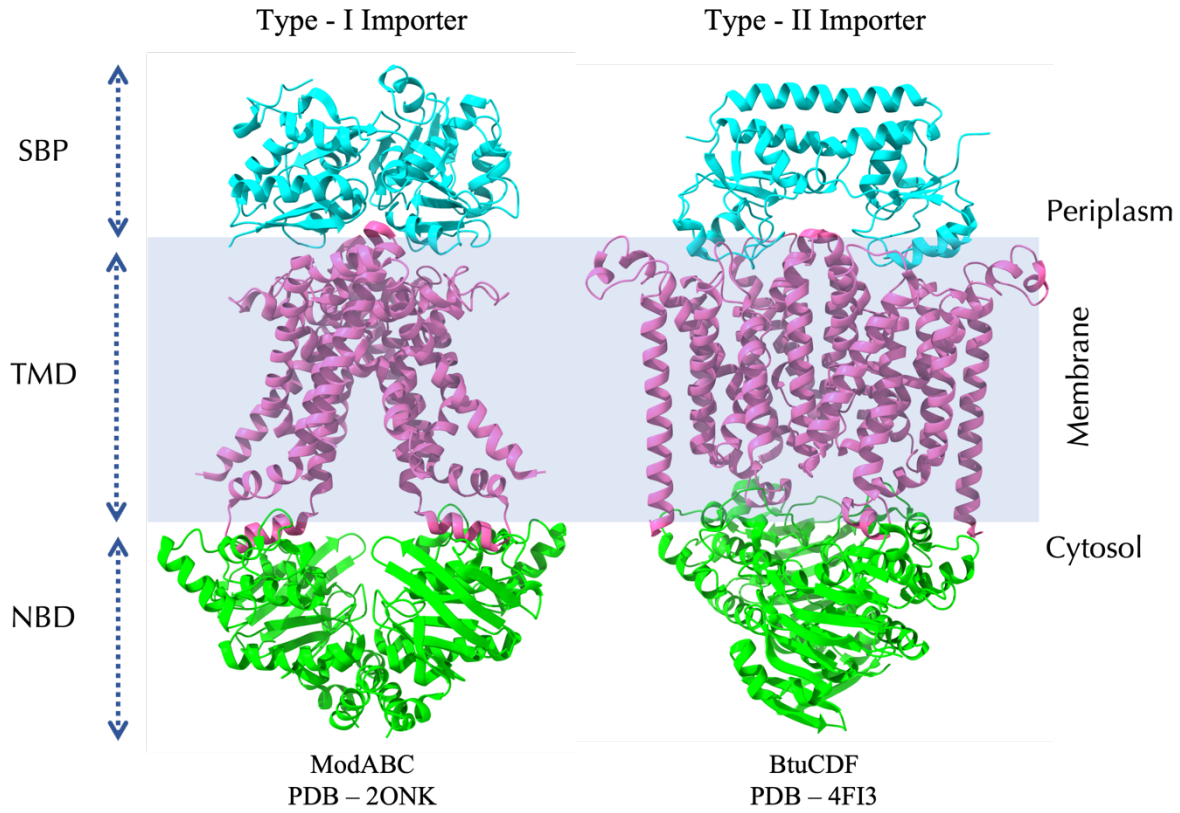

Figure 8. *Type I and II importer. The TMDs are colored hot pink, the NBDs are in lime and SBPs are in cyan.*

Type-I ABC importers:

Type I ABC importers are a type of ABC transporter that is involved in the active transport of small, hydrophobic substrate molecules, such as sugars, amino acids, and compatible solutes, across the cytoplasmic membrane[73]. The most common type-I ABC importers, such as the molybdate, maltose, and methionine systems (ModABC, MalFGK, and MetNIQ, respectively)[74-76], contain 5-8 helices per domain. Type I Importers include a periplasmic substrate-binding protein (SBP) serving as an accessory protein within the periplasmic space of Gram-negative bacterial cell. It binds to the specific substrate and brings it to the TMD for

translocation across the inner membrane. The binding of the substrate to the SBP induces a conformational change that allows it to interact with the TMD.

The TMDs of type I ABC importers like *E. coli* MalFGK and *Neisseria meningitides* MetNIQ contain a low-affinity binding site for substrate located approximately halfway through the membrane, which allows them to transport substrate molecules into the cell against a concentration gradient[76,77]. Type I ABC importers play a crucial role in maintaining cellular homeostasis by allowing cells to import essential nutrients and remove waste products[1]. For example, the Type-I ABC importer system $MalFGK_2$ in *E. coli* is responsible for the uptake of maltose and maltodextrins[78]. Maltose is an essential nutrient that *E. coli* requires for growth, and the $MalFGK_2$ system enables *E. coli* to import maltose from the external environment. Once inside the cell, maltose is broken down into glucose and used as a source of energy. Studies using biochemical, biophysical, and structural methods have captured several intermediate conformations of the maltose transporter during the transport cycle, providing insight into the mechanism of transport and the role of ATP hydrolysis in driving the process[75,79].

Type-II ABC importers:

Type-II ABC importers are involved in the active transport of large and hydrophilic substrates across the cytoplasmic membrane. Unlike type-I ABC importers, which transport relatively small and hydrophobic substrates, type-II ABC importers specialize in transporting larger molecules, such as proteins, lipids, and polysaccharides[80]. Type-II ABC importers contain additional number of transmembrane helices (10-12 transmembrane helices per domain) compared to type-I ABC importers[81]. The additional helices in type-II ABC importers are thought to be responsible for forming a large and hydrophobic transmembrane cavity that can accommodate larger substrate molecules, such as proteins and polysaccharides. The orientation of the transmembrane helices in type-II ABC importers is also important for substrate

translocation. By having all helices oriented parallel to the transmembrane cavity, type-II ABC importers create a continuous hydrophobic pathway for the substrate to traverse, allowing for efficient and specific substrate transport[81].

Type-II ABC importers have been found to be less efficient than type-I ABC importers in terms of ATP usage[82]. For example, *in vitro* studies of the type-II vitamin B_{12} transporter BtuCD have shown that it hydrolyzes approximately 100 ATP molecules per vitamin B_{12} molecule transported[70]. This inefficiency in ATP usage is thought to be due to the increased size and complexity of the substrate molecules that type-II ABC importers transport, as well as the additional energy requirements associated with substrate translocation across the cytoplasmic membrane. Despite the higher ATP requirements, type-II ABC importers still play an important role in the transport of large and hydrophilic substrate molecules, such as proteins and polysaccharides, which cannot be effectively transported by type-I ABC importers.

2.7.2 Exporters:

ABC exporters play a critical role in regulating the transport of a wide variety of substrates across the cellular membrane. Like ABC importers, ABC exporters consist of two main components: transmembrane domains (TMDs) and nucleotide-binding domains (NBDs). However, the organization of TMDs and NBDs in ABC exporters is typically different from that in ABC importers. In ABC exporters, the TMDs are usually located at the inner surface of the cell membrane, while the NBDs are located in the cytoplasm. One well-studied example of an ABC exporter is the P-glycoprotein (P-gp) transporter, which is involved in drug resistance in cancer cells[83]. P-gp is highly expressed in cancer cells, where it pumps chemotherapeutic drugs out of the cells, rendering them ineffective. P-gp consists of two TMDs and two NBDs, and it can transport a wide range of structurally diverse molecules out of the cell[84]. Another example of an ABC exporter is the multidrug resistance protein (MRP) transporter, which is involved in the detoxification of xenobiotics and drug resistance in bacteria[85]. MRP is capable

of transporting a wide range of substrates, including glutathione conjugates, glucuronides, and a variety of drugs and toxins[86].

This class of transporters is divided into two main categories based on the type of substrate transported: Type-I and Type-II exporters (Figure 9). Type-I ABC exporters are involved in the export of various proteins from the cell, including toxins, hydrolytic enzymes, S-layer proteins, lantibiotics, bacteriocins, and competence factors[87]. These exporters play an important role in maintaining cellular homeostasis and protecting the cell from environmental stressors. Type-II ABC exporters, on the other hand, play a major role in the development of antibiotic and chemotherapy resistance in bacteria and cancer cells[87]. These transporters can pump various drugs out of the cell, thereby reducing the intracellular concentration of the drug and reducing its efficacy. This has made ABC exporters an important target for the development of new antibiotics and anticancer agents. Structural analysis of prokaryotic ABC exporters has revealed a significant amount of structural diversity, much like the structural diversity observed in ABC importers. This diversity reflects the wide range of physiological processes that ABC exporters are involved in, as well as the various substrate specificities and transport mechanisms that they use.

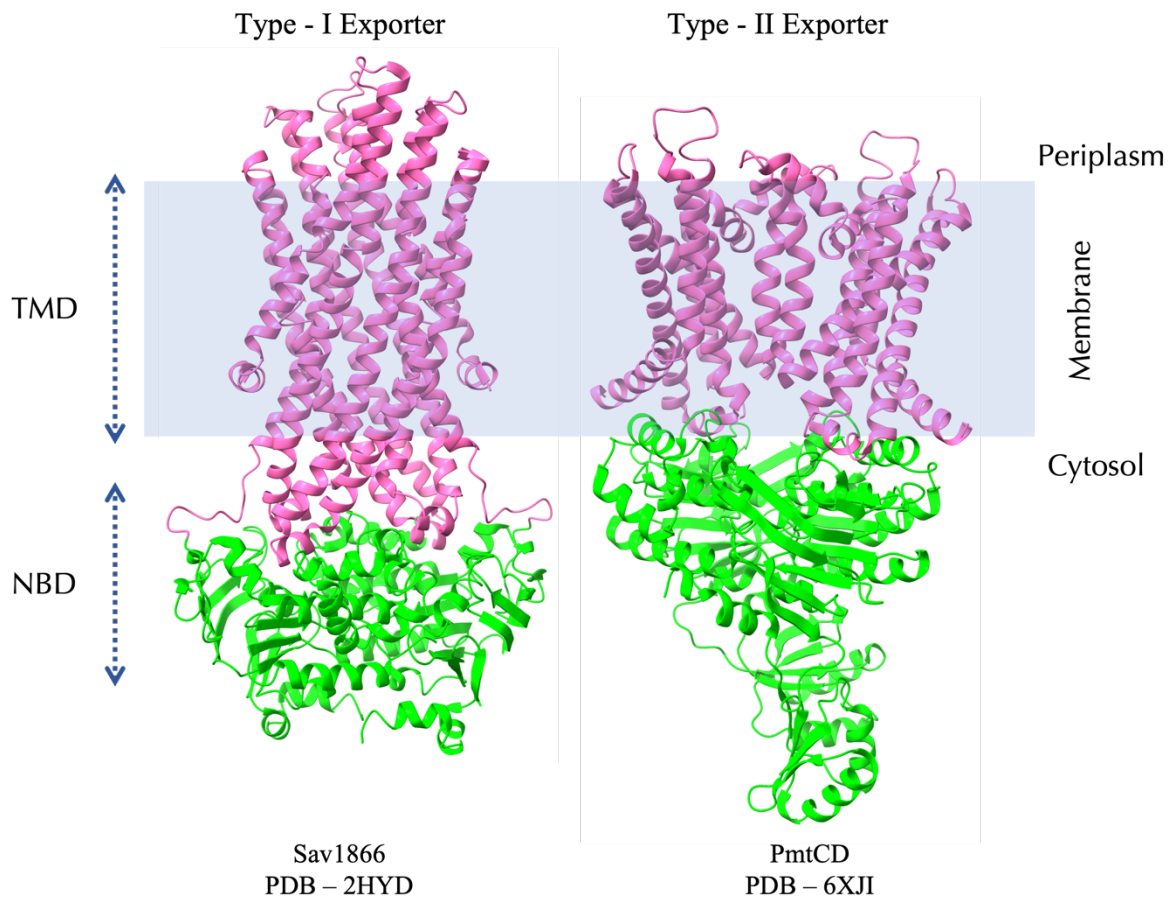

Figure 9. *Type I and II exporter. The TMDs are colored hot pink, and the NBDs are in lime.*

Type-I ABC exporters:

Type-I ABC exporters also consist of two transmembrane domains (TMDs) and two Nucleotide-binding domains (NBDs). The TMDs form a channel through which substrates are translocated, while the NBDs provide the energy required for substrate transport by hydrolyzing ATP. In this mechanism, the transporter alternates between an inward-facing conformation, where the substrate binding site is facing the cytosol, and an outward-facing conformation, where the substrate binding site is facing the extracellular environment[62] (Figure 10). Substrates bind to the transporter in the inward-facing conformation and are then transported across. Substrate transport involves conformation changes on the TMDs from the inward-facing conformation to the outward-facing conformation. ATP hydrolysis by the NBDs

provides the required energy to support these conformational changes[62]. In the typical type-1 exporter, the TMDs are responsible for recognizing and binding the substrate, while the NBDs use the energy from ATP hydrolysis to drive the transport of the precursor peptide across the plasma membrane.

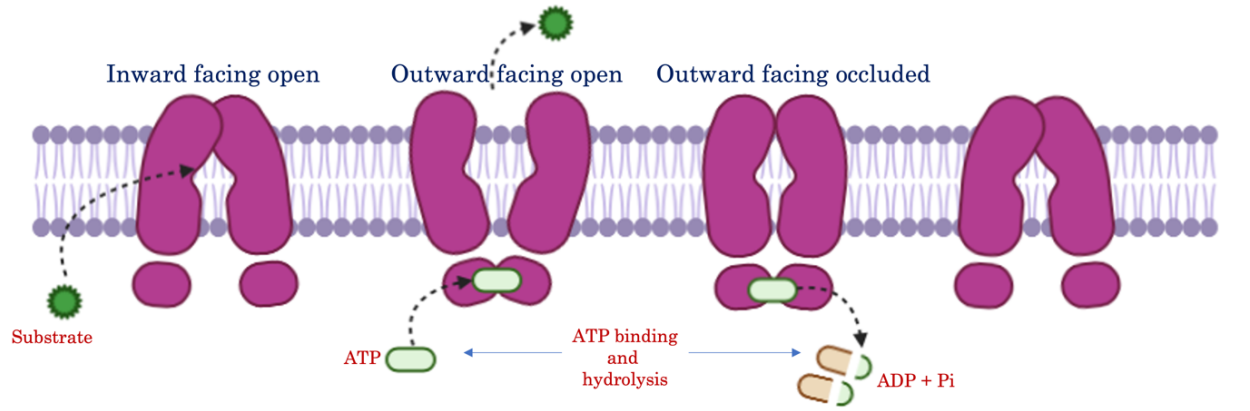

Figure 10. *ABC exporter: substrate translocation sequence. Made in BioRender.*

The type-I ABC exporter fold was first revealed through the X-ray crystallographic structure of the bacterial multidrug transporter Sav1866 (Figure 11) from *Staphylococcus aureus*[88]. This was a significant breakthrough in the field of ABC exporter research as it provided the first glimpse into the molecular action mechanism of type-I ABC exporters. The Sav1866 structure showed that type-I ABC exporters consist of two TMDs and two NBDs, arranged in a unique "double-psi" topology. This topology is characterized by two TMDs that are symmetrically arranged on either side of the two NBDs, which are located in the cytoplasm. The TMDs of Sav1866 consist of six transmembrane helices (TMH), five of which are long helices that extrude out

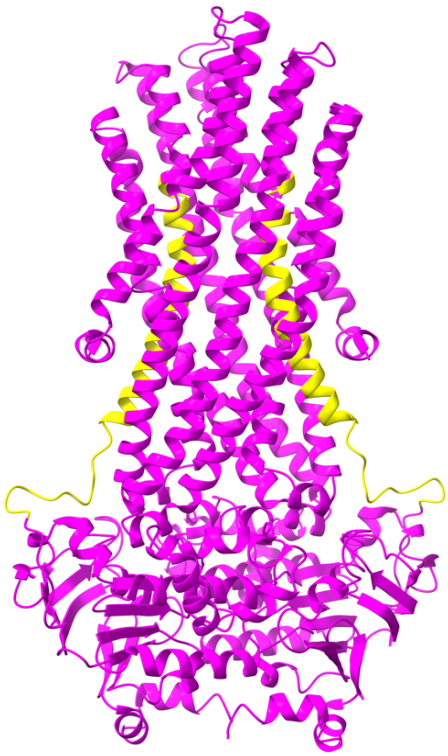

Figure 11. *Crystal structure of Sav1866 from Staphylococcus aureus. Obtained from PDB (2HYD). The sixth TMH is colored in yellow.*

from the membrane towards the NBDs. The sixth TMH is shorter and forms a loop structure within the membrane (highlighted in yellow in Figure 11). The structure of the Sav1866 multidrug transporter served as a starting point for the study of type I ABC exporters and their role in substrate transport.

Type-II ABC exporters:

Type-II ABC exporters have a different architectural design compared to type-I exporters. They contain six short transmembrane helices per transmembrane domain, and the TMDs are separated from the nucleotide-binding domains by a cytoplasmic loop region. Some examples of a type II ABC exporter are the polysaccharide transporter[89], the wall teichoic acid transporter[90], and the lipopolysaccharide transporter[91]. Type II ABC exporters have also been shown to play a role in the transport of toxic compounds, such as lytic peptides[92], and are also involved in the transport of drugs and other small molecules across the cell membrane. Therefore, understanding the transport mechanism of the type II ABC exporters is crucial for developing new strategies to combat drug resistance.

2.8 Lantibiotic secretion by ABC transporters:

Lantipeptides are a class of antimicrobial peptides produced by bacteria. Like nisin, they play an important role in the regulation of bacterial populations and defence against competitors and predators. The secretion of lanthipeptides by bacteria is mediated by ABC transporters[5]. In the case of lanthipeptides, the ABC transporter acts as a pump that exports the biosynthesized peptides from the cytoplasm to the extracellular environment, where they can exert their antimicrobial activity[6]. By controlling the levels of lanthipeptides inside the cell, the ABC transporter helps regulate the effectiveness of these peptides as antimicrobial agents[4]. In addition to their role in the secretion of lanthipeptides, ABC transporters have been the subject of diverse research due to their broad substrate specificity and their potential as targets for the

development and secretion of new antibiotics. Understanding the mechanisms by which ABC transporters mediate the secretion of lanthipeptides can provide important insights into the regulation of bacterial populations and the development of new antimicrobial targets.

Based on the bioinformatical analysis, the nisin transporter (NisT) is predicted to be a type-I ABC exporter. The prediction that NisT is a type-I ABC exporter is consistent with the known function of the protein as a nisin transporter and supports the idea that ABC transporters are well-suited for transporting modified peptides across the bacterial cell membrane. Simiar to other ABC transporters, it was suggested the TMDs of NisT are responsible for recognizing and binding the modified NisA precursor peptide, while the NBDs use the energy from ATP hydrolysis to drive the translocation process. Therefore, NisT allows the efficient and targeted export of the precursor peptide, ensuring optimal secretion of Nisin.

3. Methods:

3.1 NisT expression vector construction:

Affinity his-tagged full-length *nisT* gene from *Lactococcus lactis* (accession number: Q03203) cloned into NICE® pNZ8148 expression vector[93]. The cloning of the gene into the expression vector was performed by the Thibodeaux lab at the Department of Chemistry, McGill University.

3.2 Bacterial strains and growth conditions:

The *L. lactis* NZ9000 strain was grown in M17 medium at 30°C under semi-aerobic conditions supplemented with 0.5% glucose (GM17). For the transformation, competent cells were prepared using the protocol derived from the Nisin expression system for the *L. lactis* handbook[93]. And electroporation was used for the transformation. After transformation, cells were grown on M17 medium agar at 30°C under semi-aerobic conditions supplemented with 0.5% glucose (GM17) and chloramphenicol antibiotic at a final 10 μg/ml concentration.

3.3 Protein expression:

L. lactis NZ9000 strain was used for the homologous expression of NisT. *L. lactis* NZ9000 strain was transformed with pNZ8148-NisT and plated on GM17 agar plates containing 10 μg/ml chloramphenicol. After ~24-36 hours incubation at 30°C, 20 ml overnight culture was prepared with GM17 (10 μg/ml chloramphenicol) and incubated overnight at 30°C without shaking. 2L culture of GM17 (10 μg/ml chloramphenicol) in a 2L bottle was inoculated with the overnight culture. After optical density at 600nm (OD_{600}) reached 1.0, gene expression was induced by adding 10 ng/ml nisin (powder from Sigma-Aldrich dissolved in 50 mM lactic acid) and further grown for another 4 hours, at the end of which the cells were harvested by centrifugation at 6000 g for 15 min at room temperature. The pellets were flash-frozen in liquid nitrogen and stored at -80°C.

3.4 Protein purification:

Frozen cell pellets were resuspended in Lysis buffer (50 mM Tris-hydrochloric acid (Tris-HCl) pH 7.4, 300 mM potassium chloride (KCl), 5mM β-ME (β-mercaptoethanol) with 10 mg/ml lysozyme and protease inhibitor cocktail (Calbiochem), and incubated for 1 hr at 37°C. A total of 10 mM $MgSO_4$ and DNase I (10 ug/ml final concentration) were added and incubated for 5 min at 37°C and prior to cell lysis, cells were incubated on ice for 15 min. Cell lysis was carried out in a French press pressure cell and the lysed cell suspension was centrifuged at 11,625 g for 30 min at 4°C to remove cell debris. Subsequently, the supernatant was centrifuged at 186,009 g for 90 min at 4°C to collect the membrane fraction. Membranes were resuspended and homogenized in binding buffer (50 mM Tris-HCl pH 7.4, 300 mM NaCl, 10 mM imidazole, 5 mM β-ME). Membranes were solubilized with 1% (w/v) of the lipid-like detergents Fos-Choline-16 (FC-16) (Anatrace) for 2 hours at 4°C. Insoluble material was further removed by centrifugation at 186,009 g for 1 hour at 4°C. The supernatant was applied to a gravity Ni-NTA (Bio-Rad Econo-Column chromatography column, Thermo Scientific HisPur Ni–NTA resin) 10 ml column pre-equilibrated by binding buffer with 0.0016% (w/v) FC-16. The protein bound on the Ni-NTA resin was washed with 10 ml wash buffer 1 (20 mM Tris-HCl pH 7.4, 300 mM NaCl, 20 mM imidazole, 0.0016% (w/v) FC-16 and 5 mM β-ME), 10 ml wash buffer 2 (20 mM Tris-HCl pH 7.4, 1 M NaCl, 40 mM imidazole, 0.0016% (w/v) FC-16 and 5 mM β-ME), 10 ml wash buffer 3 (20 mM Tris-HCl, 200 mM NaCl, 50 mM imidazole, 0.0016% (w/v) FC-16 and 5 mM β-ME, pH 7.4) and eluted with elution buffer (20 mM Tris-HCl, 200 mM NaCl, 500 mM imidazole, 0.0016% (w/v) FC-16 and 5 mM β-ME, pH 7.4). The eluted fractions (1.5ml each) were pooled and further concentrated by an Amicon® Ultra 100 kDa molecular weight cut-off spin concentrator. The protein was then applied onto a size exclusion column (SEC) (Superose 6 increase 10/300 GL, Cytiva) pre-equilibrated with 10 mM Tris-HCl pH 7.4, 200 mM NaCl, 0.0016% (w/v) FC-16 and 5 mM β-ME. For detergent

exchange, the eluted protein from the Ni-NTA column was buffer exchanged to 0.02% n-Dodecyl-B-D-Maltoside (DDM) (Anatrace) using a spin concentrator and injected onto a size exclusion column (Superose 6 increase 10/300 GL, Cytiva) pre-equilibrated with 10 mM Tris-HCl pH 7.4, 200 mM NaCl, 0.02% (w/v) DDM and 5 mM β-ME, pH 7.4. The main peaks fractions were analyzed by sodium dodecyl-sulphate polyacrylamide gel electrophoresis (SDS-PAGE) and purified proteins were further concentrated by a spin concentrator. The final protein concentration in detergent micelles was measured by recording the absorbance at 280 nm.

3.5 Peptidisc reconstitution:

3.5.1 *Preparation of Nanodisc scaffold protein reversed (NSPr):*

Peptidisc also known as peptide NSPr (N'-FAEKFKEAVKDYFAKFWDPAAEKLKEAVK DYFAKLWD-C') was purchased from Peptidisc Biotech. The peptide was solubilized to 5 mg/ml in 20 mM Tris-HCL pH 7.4 and 200 mM NaCl.

3.5.2 *In-gel reconstitution*:

The target membrane protein NisT (1 μM) was mixed with increasing concentrations of peptidisc (0-65 μM) and allowed to incubate for 1-2 minutes at room temperature. The mixture was then supplemented with buffer A (20 mM Tris-HCL pH 7.4 and 200 mM NaCl) to bring the final detergent concentration below its critical micelle concentration (CMC) while keeping the final volume to 15 μl. A solution of glycerol was added to 10% final to facilitate loading on 4-12% clear native polyacrylamide gel electrophoresis (CN-PAGE). The electrophoresis was set constant at 25 mA for 1 hour at room temperature and then the bands were visualized by Coomassie Blue G250 staining.

3.5.3 *On-column reconstitution*:

The target membrane protein NisT and peptidisc were mixed in a 1:15 molar ratio in a total volume of 100 μ L in buffer A. The mixture was immediately injected into a Superdex 200inc column (10/300 GL, Cytiva) pre-equilibrated with 10 mM Tris-HCl pH, 200 mM NaCl, and 2 mM β-ME. Desired fractions were collected and visualized by SDS-PAGE.

3.6 ATPase activity assay:

The ATPase activity of purified and detergent-solubilized NisT was measured using the ADP-Glo Max assay (Promega). The ATPase reaction was performed using 1X reaction buffer at a final concentration of 20 mM Tris-HCl pH 7.4, 100 mM NaCl, 10 mM $MgCl_2$, and 0.013% of DDM or FC-16. The enzymatic reaction was performed at room temperature for 40 minutes and was stopped by the addition of ADP-Glo^{TM} Max detection reagent to convert ADP to ATP and introduce luciferase and luciferin and allow ATP detection. The quenched samples were further incubated at room temperature for 60 minutes and measured by a plate-reading luminometer (GloMax® discover microplate reader, Promega). All the reactions were carried out in triplicates and ATPase rates were determined using linear and non-linear regression to the Michaelis–Menten equation in GraphPad Prism (Version 9 software).

3.7 Electron microscopy (EM) grid preparation:

For negative stain EM, copper grids coated with carbon (CF400-CU) were glow discharged at 15 mA for 30 seconds using a Pelco easiGlow Glow Discharge unit. 5 µl of protein sample was applied to the grid, incubated for 1 min at room temperature and excess liquid was then removed by blotting. The grid was washed one time by placing the grid on a 30 µl droplet of deionized water for 5 seconds and excess water was removed by blotting. The grid was stained by placing on a 30 µl droplet of 2% w/v uranyl acetate solution for 5 seconds, followed by blotting, and then placing on a second 30 µl droplet of 2% w/v uranyl acetate solution for 1

min before final blotting. Grids were kept for another 10 minutes to dry completely and stored until imaging.

For cryo-EM, C-flat holey carbon-coated grids (Quantifoil 300 mesh, 1.2/1.3) were glow discharged at 10 mA for 20 seconds and mounted in an FEI Vitrobot MkIV set to 100% humidity at 4°C. 5 µl of ~5mg/ml purified protein were applied to the grids and left to absorb for 3 seconds, then blotted for 3 seconds with 1 blot force. After blotting, grids were frozen by plunging into liquid ethane, cooling the sample fast enough to prevent the formation of crystalline ice. Also, to capture the NisT transporter in an ATP-bound state, an ATP analog such as adenosine 5'-O-(3-thiotriphosphate) (ATPγS) was used in 1:5 molar ratio (NisT:ATPγS). The ATPγS was mixed with NisT just before freezing grids (1:5 molar ratio NisT:ATPγS). And all grids were frozen with the same freezing condition described above. After freezing, grids were stored in liquid nitrogen until imaging.

3.8 EM imaging and data collection:

Negatively stained grids were imaged on an FEI Tecnai G2 Spirit Twin transmission electron microscope (TEM) at 120 kV at 68,000x magnification with a Gatan Ultrascan 4000 4k x 4k CCD Camera. Cryo-EM grids were screened to assess protein aggregation state, particle density and ice quality using an FEI Tecnai G2 F20 TEM operating at 200 kV with a TVIPS TemCam XF416(ES) 16MP CMOS Camera. Suitable samples were then forwarded to full data collection in the FEI Titan Krios microscope operated at 300 kV. For data collection, the Gatan K3 direct detection camera was used in counting mode at 130,000x magnification with a defocus range of -1.00 to -2.50 µm (interval 0.25 µm), which produced images with a calibrated pixel size of 0.675Å with two electrons per frame. Four different data sets were collected i.e., (i) NisT+FC-16_noATP, (ii) NisT+FC-16_ATPγS, (iii) NisT+DDM_noATP, and (iv) NisT+DDM_ATPγS. And all datasets were collected with the same parameters described above.

3.9 Image processing:

Two different data processing software has been used for this project i.e., RELION 4.0[94] and cryoSPARC v4.0[95]. Motion correction and dose weighting were performed using MotionCor[96] implemented in both RELION and cryoSPARC. Contrast transfer functions were then calculated using CTFFIND4[97]. Particle picking and initial particle extraction were carried out in both RELION and cryoSPARC. Subsequent data processing is described in later chapters.

3.10 Hydrogen–deuterium exchange mass spectrometry (HDX-MS) sample preparation:

Reference/Undeuterated sample preparation (control):

To prepare the control samples in a non-deuterated buffer, NisT purified with two different detergents (FC-16 and DDM) was concentrated to 5 μM after SEC purification using 0.5 mL Amicon® Ultra 100 kDa molecular weight cut-off spin concentrator. Then the NisT was diluted to a final concentration of 2 μM in reaction buffer 1 containing 10 mM Tris-HCL pH 7.4, 200 mM NaCl, 0.0016% FC-16 and reaction buffer 2 containing 10 mM Tris-HCL pH 7.4, 200 mM NaCl, 0.02% DDM to a final volume of 50 μL. Each reaction was prepared in triplicate. Then the reactions were quenched immediately by adding 75 μL of quench buffer (100 mM sodium phosphate and 0.8 M guanidine HCl (pH 1.7)) to give a final pH meter reading of 2.1. Quenched samples were immediately flash-frozen in liquid nitrogen and stored at −80 °C until Liquid chromatography–mass spectrometry (LC−MS) analysis.

Deuterated sample preparation:

NisT purified with DDM was first concentrated to 20 μM using 0.5 mL Amicon® Ultra 100 kDa molecular weight cut-off spin concentrator. To initiate the HDX reaction, NisT was diluted to a final concentration of 2 μM in HDX reaction mixtures containing 10 mM Tris-HCL pD 7.0, 200 mM NaCl, 1 mM AMP-PNP (when present), 1 mM ATP (when present), 10 μM NisA (when present) to a final volume of 50 μL. Each reaction was prepared in triplicate. Then the

HDX reactions were quenched after incubating for 30 minutes by adding 75 µL of quench buffer (100 mM sodium phosphate and 0.8 M guanidine HCl (pH 1.7)) to give a final pH meter reading of 2.1. Quenched samples were immediately flash-frozen in liquid nitrogen and stored at −80 °C until Liquid chromatography–mass spectrometry (LC−MS) analysis.

3.11 Mass Spectrometry Data Collection and Analysis:

Frozen 125 µL of quenched reaction aliquots were thawed in a 30 °C water bath for 65 seconds before being injected into a Waters immobilized pepsin column using a 40 µL injection loop of the HDX manager. The immobilized pepsin column was held at 15°C or 20°C to optimize the right condition and then the sample was passed through the pepsin column with 0.1% formic acid in H_2O at a flow rate of 100 µL/min. For the sample optimization, two different time points were used for the digestion phase i.e., 3 min or 5 min. After a 3 min or 5 min digestion phase, the peptides were eluted from the trap column onto a Waters BEH C18 UPLC column (equilibrated in 95:5 (v/v) H2O: acetonitrile, 0.1% FA) and separated at 0.4°C with a linear gradient of 5–40% in 13 min and then four alternative cycles of 5% and 95% until 25 min. The sample was then ionized by electrospray ionization (ESI) using the following source settings: capillary voltage of 2.8 kV, sampling cone = 30 V, source offset = 30 V, and desolvation temperature = 175 °C. And the data were collected in positive ion and resolution modes in the m/z range of 100-2000. All mass spectrometry was performed on a Waters Synapt G2-Si with HDX technology. For the identification of non-deuterated peptides, data were collected in MS^E mode, and the resulting peptides were identified using PLGS™ software (ProteinLynx Global SERVER 3.0.2 from Waters™).

4. Results:

4.1. Protein expression and purification

4.1.1. NisT expression optimization:

Conditions supporting the optimal expression of NisT were screened. The condition screening included cell density alteration at induction point and alteration of the inducer concentration. Variation in cell density at the time of indication identified that $OD_{600\ nm}$ 1.0 is the optimal cell density, due to the NisT expression compared to $OD_{600\ nm}$ and with minimal degradation products compared to $OD_{600\ nm}$ 1.5, see SDS-PAGE analysis in Figure 12.

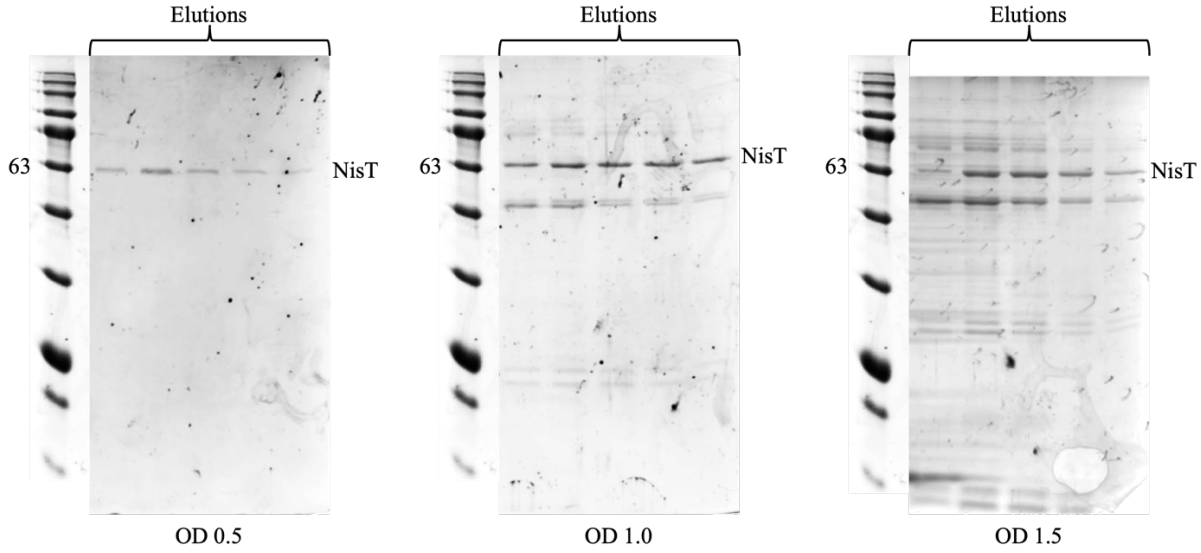

Figure 12. *NisT expression test at different induction time. Coomassie-stained SDS-PAGE analysis after Ni-NTA purification shows a protein band at 63kDa protein marker.*

Different Nisin (protein expression inducer) concentrations of 10 ng/ml, 20 ng/ml and 30 ng/ml were also screened to examine if a higher amount of nisin could enhance protein expression. The SDS-PAGE gel analysis showed no significant increase in protein expression even after increasing the Nisin concentration (Figure 13). As such, 10 ng/ml Nisin was used in all further experiments.

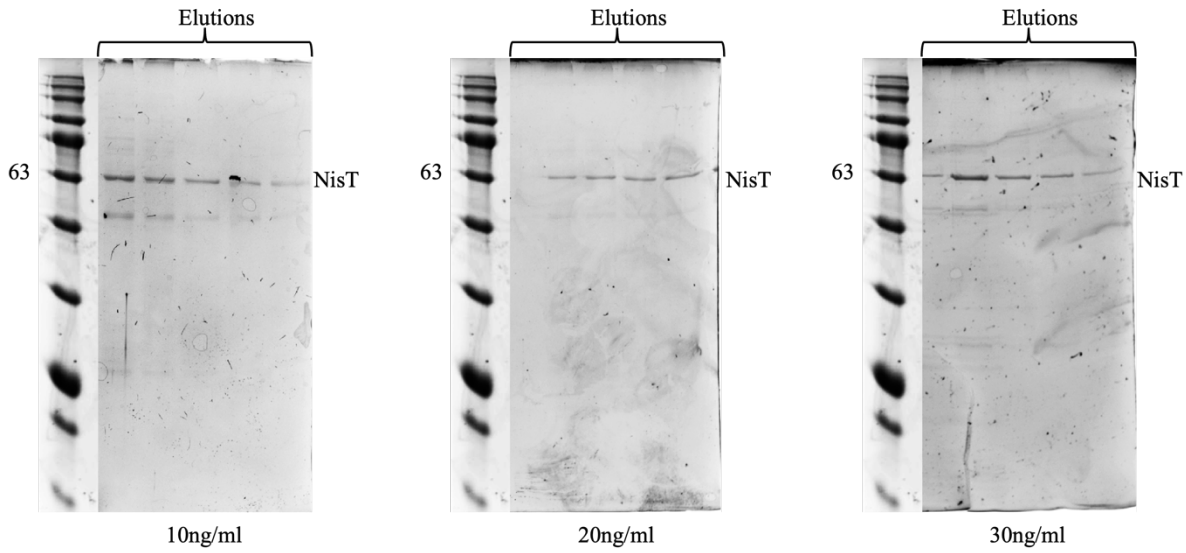

Figure 13. *NisT expression test at different nisin concentration. Coomassie-stained SDS-PAGE analysis after Ni-NTA purification shows a protein band at 63kDa protein marker.*

4.1.2. NisT purification:

In any biochemical project, it is often necessary to express and purify significant quantities of protein. The plasmid utilized for NisT expression contained the *nisT* gene, fused to a ten-histidine residue (10HNisT) tag at the C-terminus of the *nisT*. 10HNisT was homologously expressed in *L. lactis* NZ9000 (typically, resulting in 9 grams of cell from a 2 L culture). Initially, NisT was extracted from the membranes by 1% dodecyl maltoside (DDM) detergent due to its mild protein denaturation properties. Unfortunately, DDM was unable to efficiently extract NisT as evident by the elution of the DDM-extracted protein in the void volume of a size-exclusion chromatography (SEC), suggesting that the protein aggregated (Figure 14).

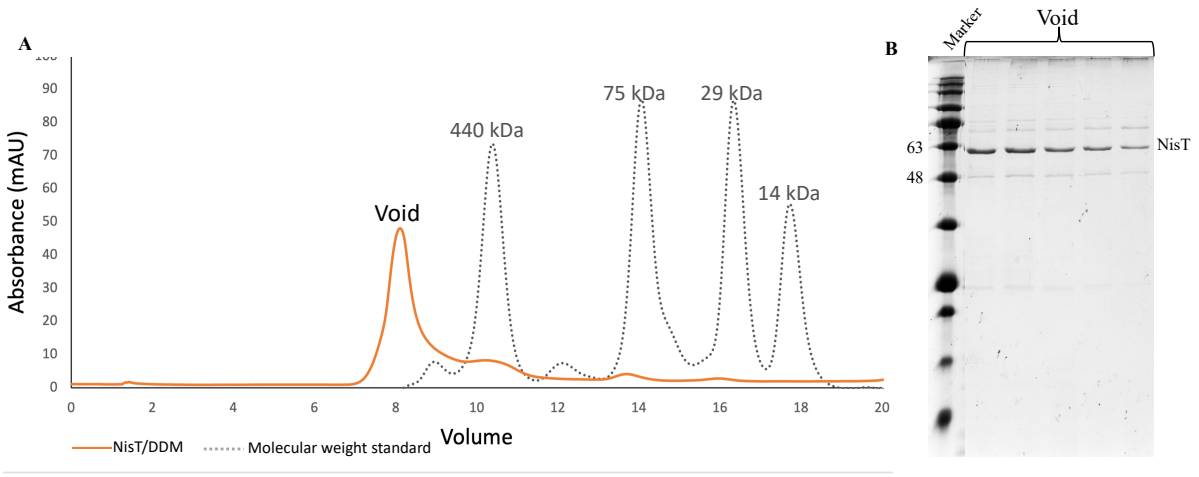

Figure 14. *Purification of NisT in DDM. (A) SEC chromatogram of 10HNisT displayed a void peak at 8 ml on a Superdex 200increase 10/300 GL column. Molecular markers, ferritin (440 kDa), conalbumin (75 kDa), carbonic anhydrase (29 kDa) and ribonuclease A (14 kDa), are indicated by a dashed gray line. (B) A typical Coomassie-stained SDS-PAGE gel shows a protein band between 48 and 63kDa protein marker.*

A previous study reported that 1% Fos-choline 16 (FC-16, Anatrace) detergent could be used to solubilize and purify NisT[5]. So, in our experiment, 10HNisT was similarly solubilized with the FC-16 and purified by immobilized metal ion affinity (IMAC) followed by SEC. Similar to other membrane proteins[98-100], 10HNisT (69 kDa) showed higher mobility on the SDS-PAGE gel and migrated to a distance that approximately corresponds to 60 kDa (Figure 15B). 10HNisT eluted from SEC both in the void peak and in a volume that corresponded to a dimer in detergent micelle (Figure 15A). Subsequently, the dimeric 10HNisT elution fractions were further concentrated and used for ATPase activity assay, peptidisc reconstitution and structural studies.

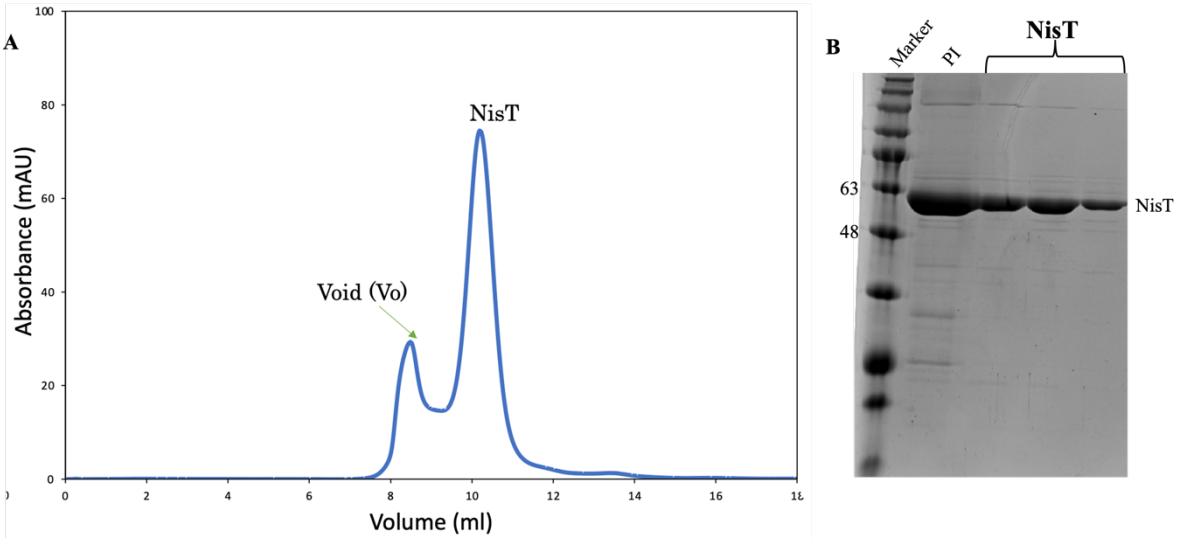

Figure 15. *Purification of NisT. (A) SEC chromatogram of 10HNisT displayed a peak (#) at 10 ml on a Superdex 200increase 10/300 GL column, (B) A typical Coomassie-stained SDS-PAGE gel shows a protein band between 48 and 63kDa protein marker.*

Since the zwitterionic detergents such as FC-16 are considered harsher surfactants than the non-ionic detergents, 10HNisT was further screened with different non-ionic detergents such as DDM, n-Undecyl-Beta-Maltoside (UDM), Lauryl Maltose Neopentyl Glycol (LMNG), Cyclohexyl-Methyl-β-D-Maltoside (CYMAL-7) and N, N-Dimethyl-n-dodecylamine N-oxide (LDAO). All the different detergents were exchanged individually on the Superdex 200increase 10/300 GL column. Among these screened detergents, only DDM was found to stabilize the protein in a volume corresponding to a dimer within a micelle (Figure 16). Accordingly, DDM exchanged 10HNisT was used for ATPase activity assay and structural studies.

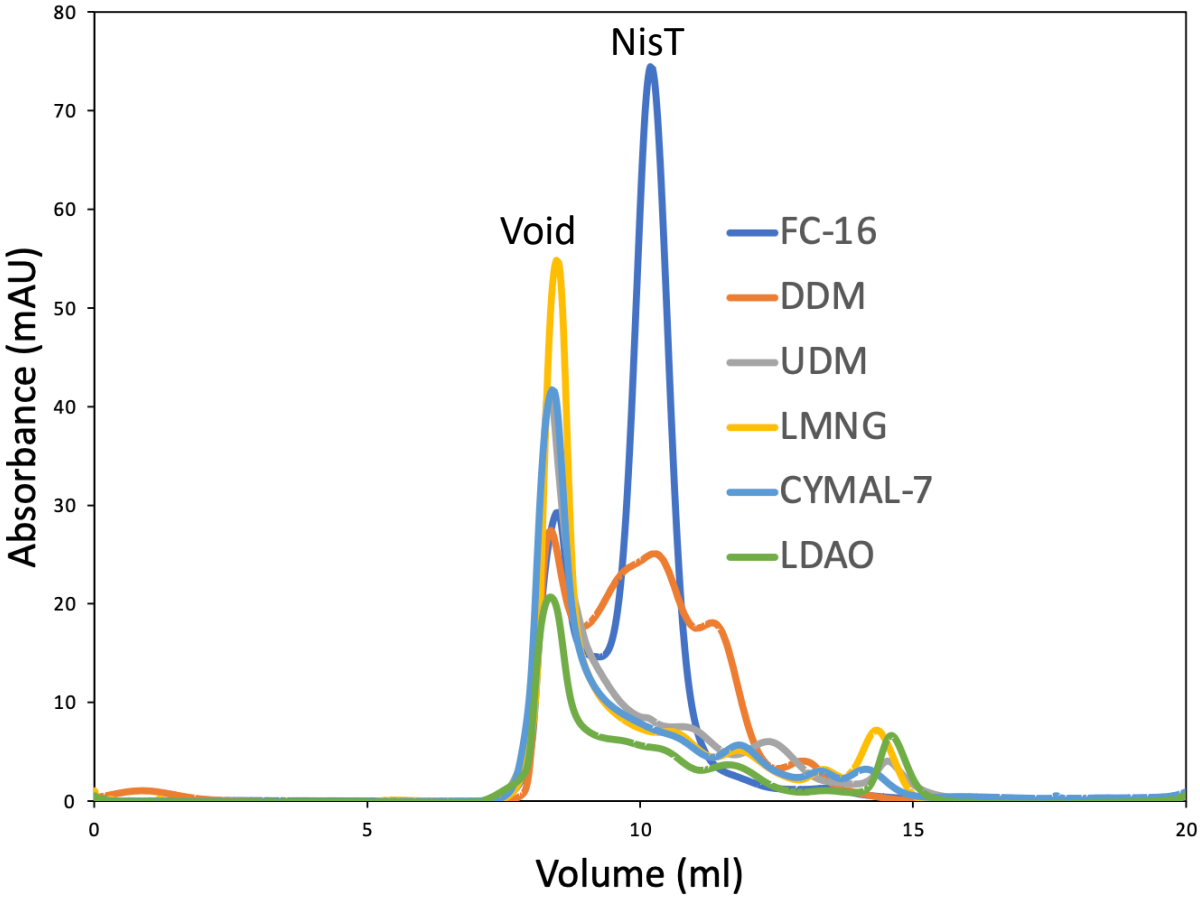

Figure 16. *Detergent screening of 10HNisT on a Superdex 200increase 10/300 GL column after solubilized in FC-16 and purified by Ni-NTA chromatography.*

Previous studies have shown that the choice of detergent can affect the structural and functional properties of membrane protein as well as the presence of high detergent concentration can result in an empty detergent micelle which increases the background noise in EM images[101]. In order to avoid and overcome this problem, membrane mimetics systems such as nanodisc[102], peptidisc[103], saposinA[104], SMALPS[105] and liposomes[106] are often used. Here we have chosen to reconstitute 10HNisT into the peptidisc membrane mimetics system.

4.2. Peptidisc reconstitution

4.2.1. In gel reconstitution:

The 'in-gel' method is a good option to determine optimal reconstitution conditions in a time- and cost-effective fashion. The target membrane protein NisT (1 μM) was mixed with increasing concentrations of peptidisc (0-65 μM) for reconstitution and ran on a blue native polyacrylamide gel electrophoresis (BN-PAGE). The expected molecular size of the 10HNisT and peptidisc complex was ~240 kDa. Unfortunately, the protein was found to aggregate in each condition tested (Figure 17).

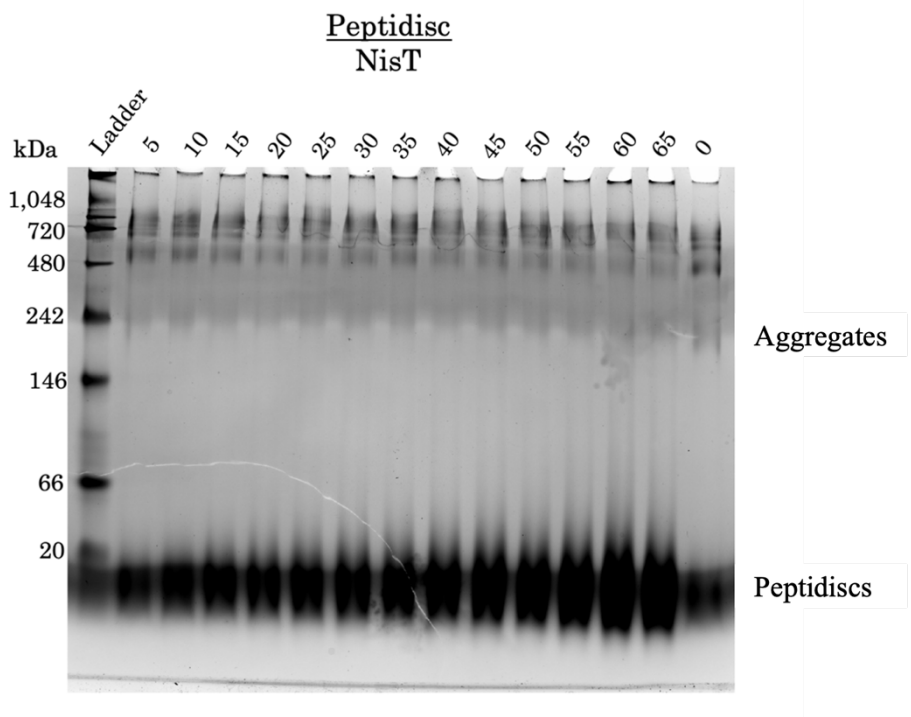

Figure 17. *On-Gel NisT/Peptidisc reconstitution (Peptidisc and NisT were mixed at the indicated molar ratio)*

4.2.2. On column reconstitution:

Since protein aggregation was observed in the in-gel reconstitution method, the on-column reconstitution method was also attempted. The resulting chromatogram is shown in Figure 18A and its fractions were analyzed by 12% SDS PAGE (Figure 18B). The analysis presented in

Figure 18 shows that the NisT reconstituted peptidisc complex fractions were both of high purity and homogeneity.

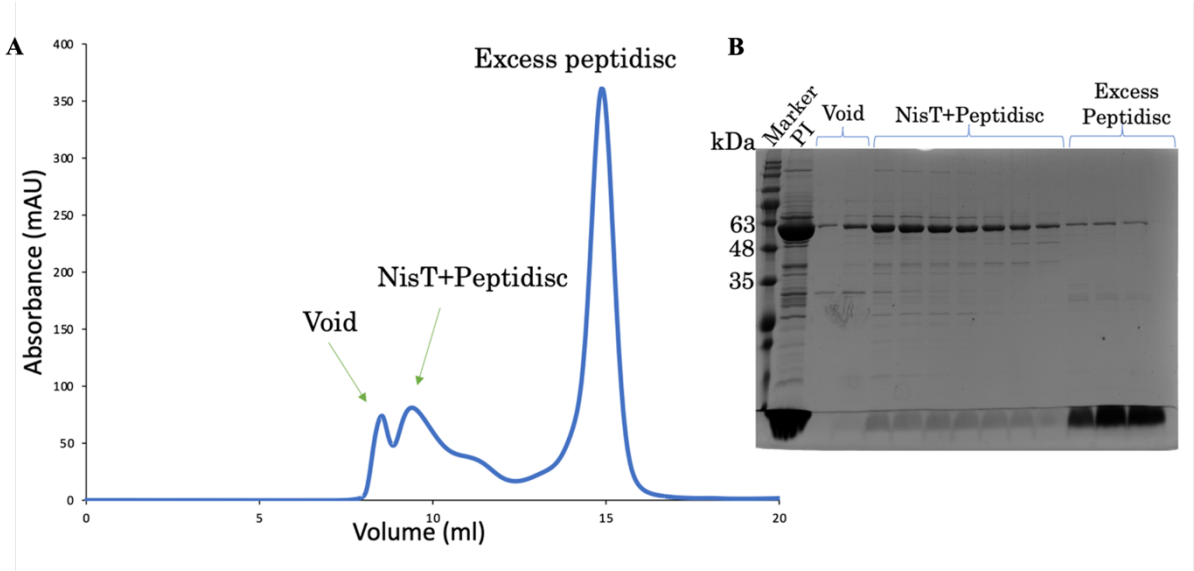

Figure 18. *On-column NisT/Peptidisc reconstitution (a) Size-exclusion chromatography profiles of NisT reconstituted into peptidiscs using the 'on-column' method. (b) 12% SDS-PAGE analysis of NisT in peptidisc. Peptidisc runs at the bottom of the gel and can be visualized with Coomassie blue staining.*

Since the protein purification protocol has been established, we then continued to examine the protein folding and activity by an ATPase assay.

4.3. <u>ATPase assay of NisT:</u>

Since ATP hydrolysis is the hallmark of a functional ABC transporter-mediated substrate translocation, an ATPase activity of NisT *in vitro* without the nisin substrate was performed. The ATPase activity was measured in both FC-16 and DDM detergent solutions using the ADP-Glo max assay kit (Promega). First, a protein concentration optimization assay was performed to determine the optimal protein concentration for the ATPase assay. For this optimization assay, a constant concentration of ATP was maintained (3 mM) in all reactions, while the concentration of NisT was varied from 0 to 6 µM. The results have clearly indicated a concentration-dependent activity of the NisT transporter was observed (Figure 19).

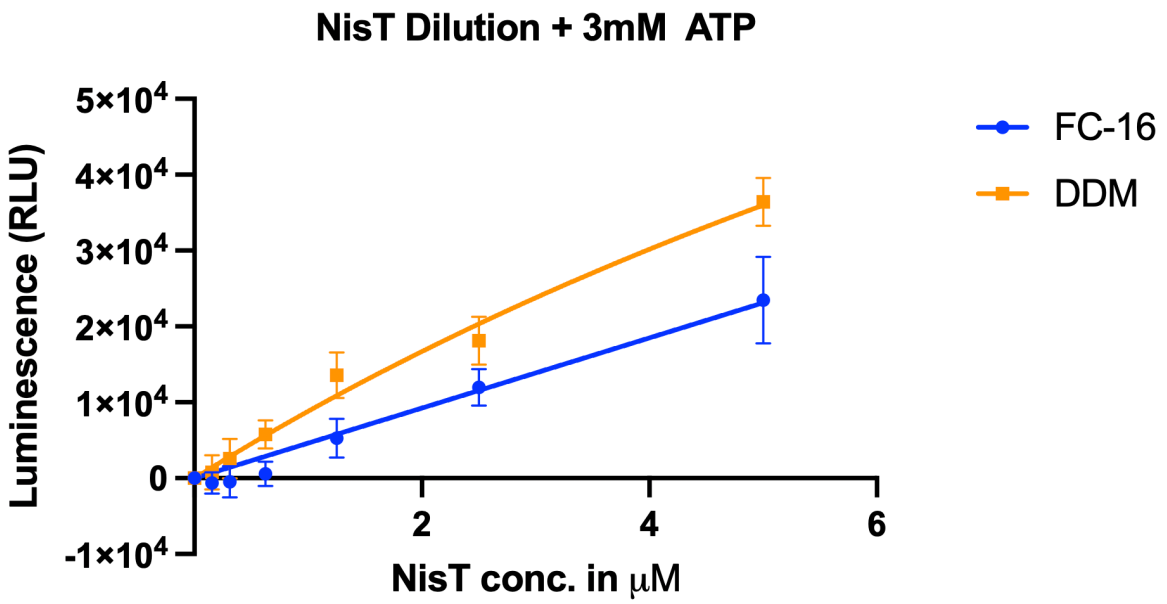

Figure 19. *NisT concentration optimization assay in varying NisT concentrations. The result was fitted using Prism GraphPad.*

After determining the optimal protein concentration, an ATPase assay was performed. In this ATPase assay, a constant concentration of NisT was maintained (5 μM) while the concentration of ATP was varied from 0 to 3 mM. The ATPase activity of NisT in both FC-16 and DDM detergents was measured using the ADP-Glo max assay kit (Promega) in the absence of a nisin substrate. To determine the kinetic parameters of NisT enzyme-catalyzed reaction, the Michaelis-Menten equation is fitted to experimental data using Prism GraphPad software. The software uses nonlinear regression analysis to fit the equation to the data and determine the values of Km. The Km value is a measure of the affinity of an enzyme for its substrate, and it provides important information about the enzymatic activity of the protein[107].

In the presence of the FC-16 detergent, the Km value of NisT was found to be 86.23μM, indicating that the enzyme has a high affinity for its substrate, ATP. In contrast, the Km value of NisT was found to be 372.3 μM in the presence of the DDM detergent, indicating a lower affinity for the substrate (Figure 20). The differences in the Km values between the two

detergents suggest that they may have different effects on the conformation and activity of NisT. This observation stands in good agreement with the knowledge that different detergents can alter the structure and function of membrane proteins[108]. In conclusion, the observed ATP hydrolysis increased as a function of the ATP concentration, suggesting that the purified protein is indeed active.

After successfully validating NisT activity in both DDM and FC-16 detergents, structural studies were commenced.

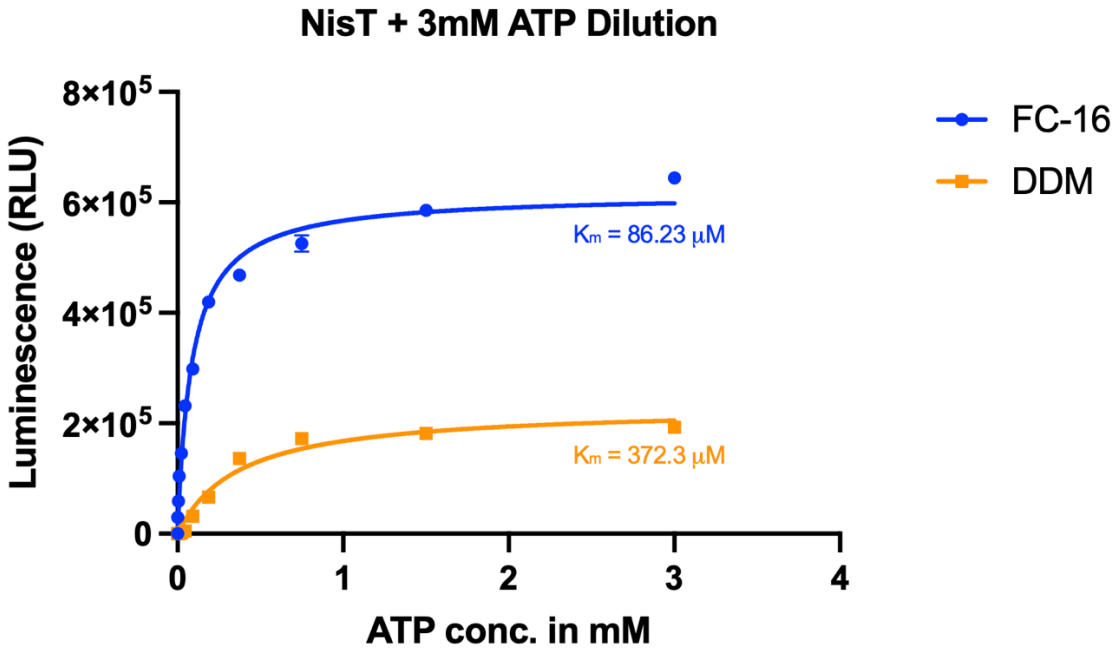

Figure 20. *ATPase assay of NisT in varying ATP concentrations. The specific ATPase rate of purified NisT was measured using the ADP-GloMax kit (Promega) and plotted against ATP concentration (mM) to determine kinetic parameters. The ATPase rate was fitted by Michaelis–Menten equation to determine the Km using Prism GraphPad software.*

4.4. NisT cryo-EM data collection:

Zwitterionic detergents like FC-16 can have varying effects on the structural integrity of membrane proteins[101]. For example, they can alter the orientation and packing of lipid molecules in the membrane, which can in turn affect the conformation and stability of the

protein[109]. Additionally, the specific properties of the detergent, such as its hydrophobicity and size, can also influence its interactions with the protein and potentially cause changes to its structure[109]. Therefore, non-ionic detergent like DDM was also used in this study. Since NisT was purified individually in both detergents, the sample quality was visualized and assessed by negative staining in TEM (Figure 21). Since the protein is in a detergent micelle, it was difficult to distinguish between a protein that was incorporated into a micelle vs an empty micelle. Also, the sample was very difficult to see on the grid due to its relatively small in size. But the samples seemed to be mostly monodispersed and therefore we continued to cryo-EM grid screening.

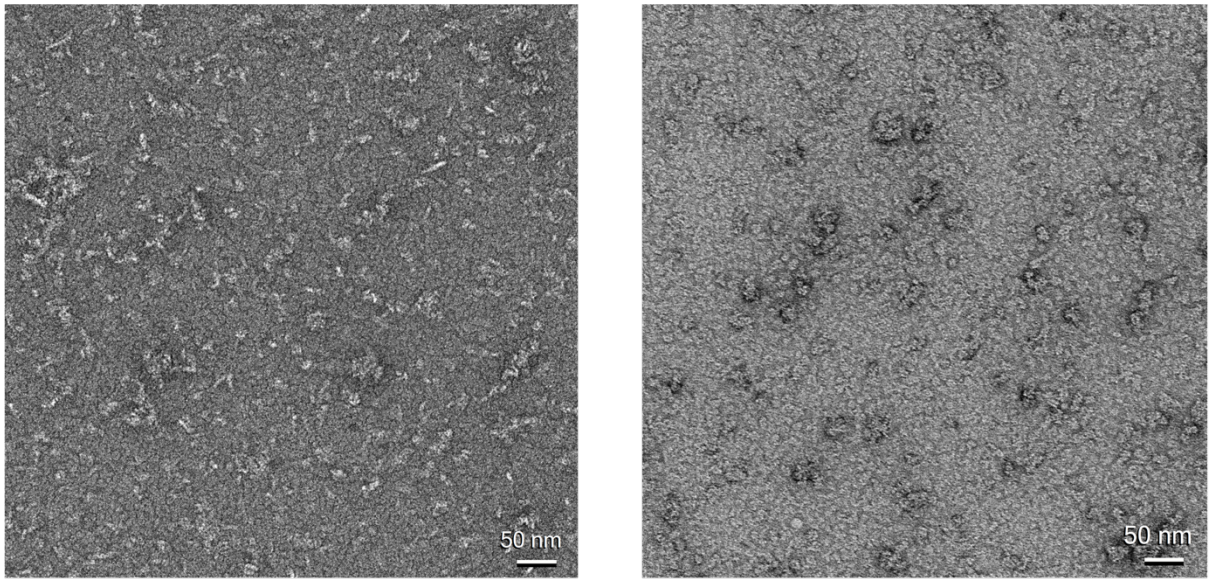

Figure 21. *Negative staining micrograph of NisT in FC-16 and DDM detergents.*

Initially, the cryo-EM samples were prepared using the CF-2/1-Cu300M grid. During grids screening in the Tecnai TF-20 TEM microscope, an uneven particle distribution was observed in both FC-16 (Figure 22) and DDM grids (Figure 23), where the protein particles were concentrated around the edge of the hole.

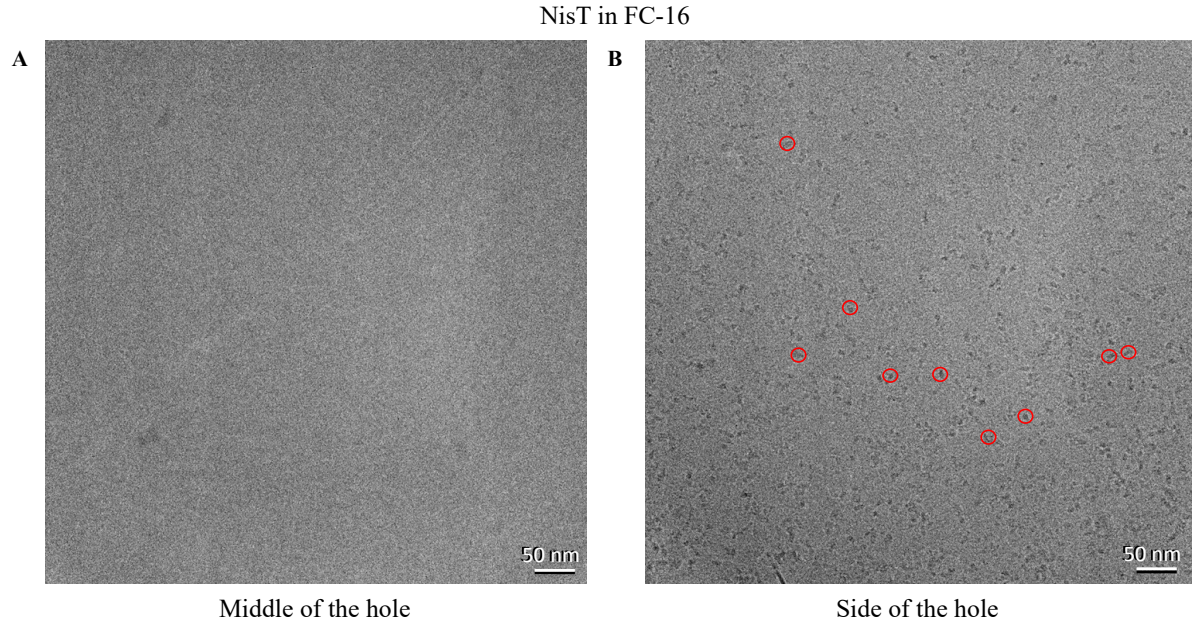

Figure 22. *Single particle cryo-EM micrograph of NisT in FC-16 grid. (A) shows no particle in the center of the hole (B) shows particles (in red circles) on the side of the hole.*

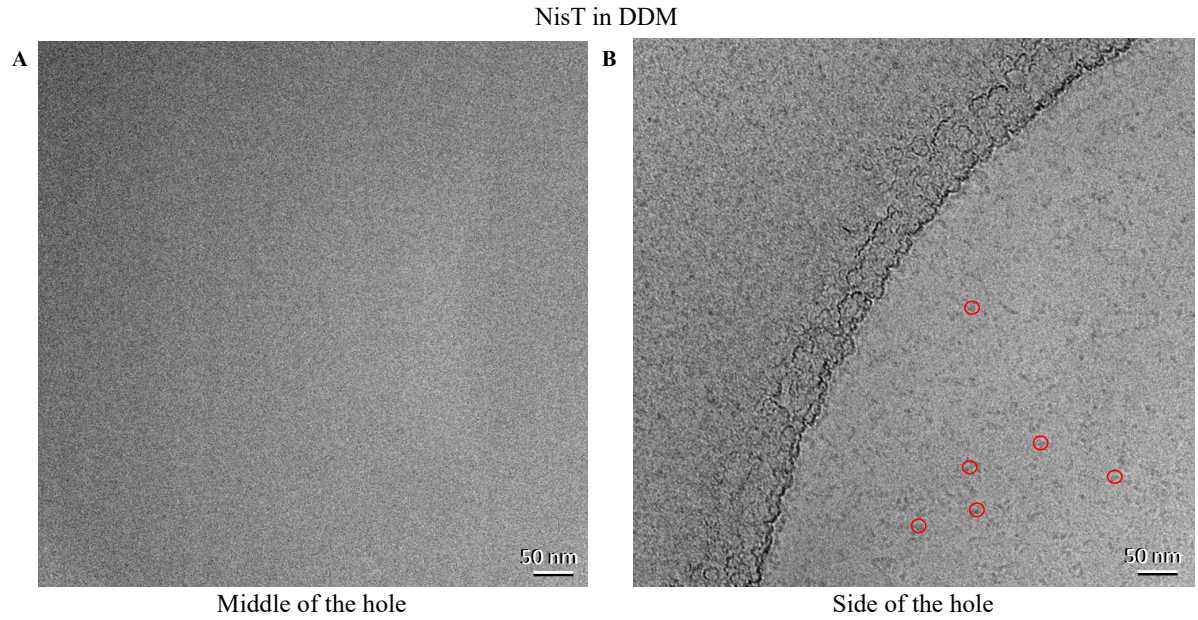

Figure 23. *Single particle cryo-EM micrograph of NisT in DDM grid. (A) shows no particle in the center of the hole (B) shows particles (in red circles) on the side of the hole.*

Hence, grids with smaller mesh sizes such as CF-1.2/1.3-Cu300M were used to minimize the effects of the uneven particle distribution. These grids have smaller holes, which

reduced the likelihood of protein particles being pushed toward the edges[110] can be seen in Figures 24 and 25.

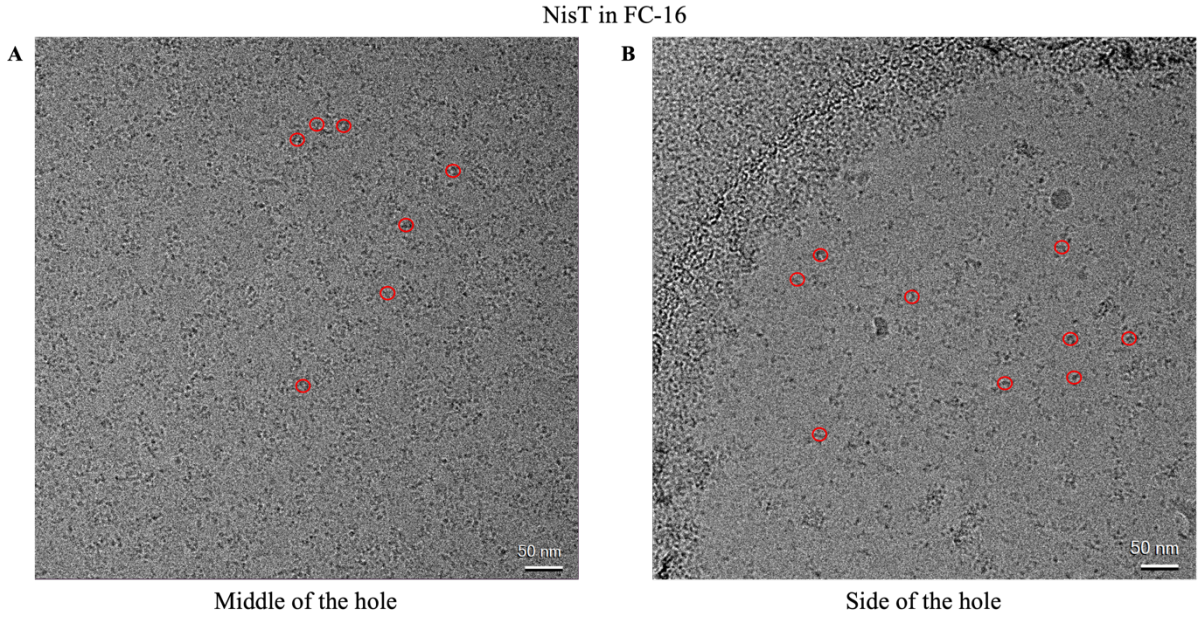

Figure 24. *Single particle cryo-EM micrograph of NisT in FC-16 grid. (A) shows particle (in red circles) in the center of the hole (B) shows particles (in red circles) on the side of the hole.*

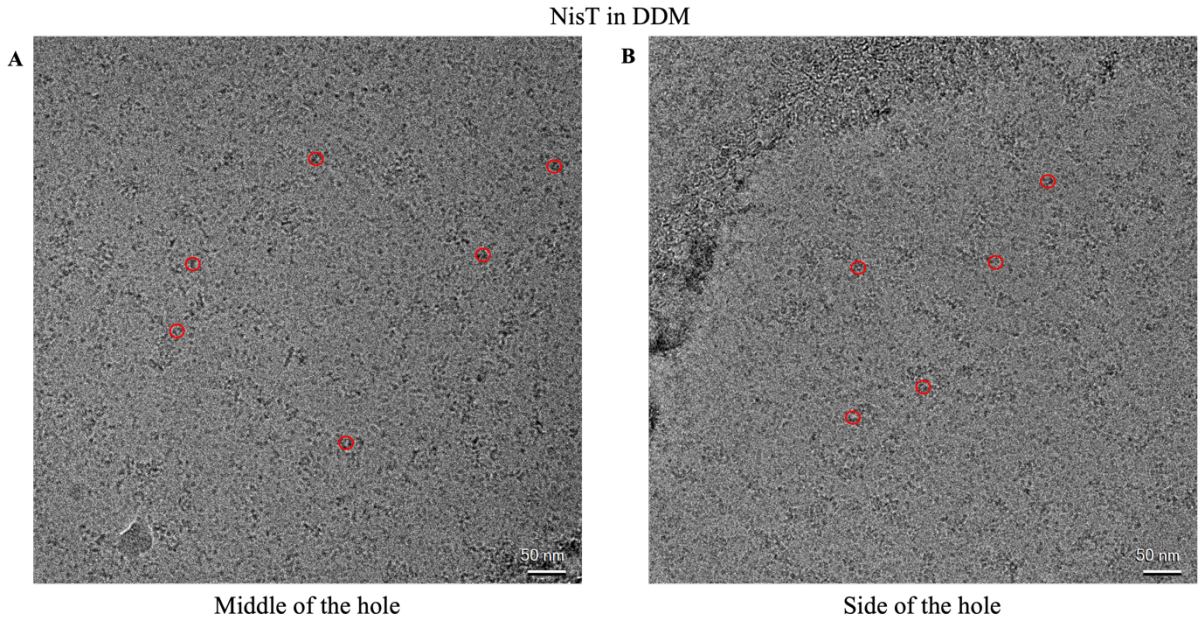

Figure 25. *Single particle cryo-EM micrograph of NisT in DDM grid. (A) shows particle (in red circles) in the middle of the grid (B) shows particles (in red circles) on the side of the grid.*

Since NisT is an ABC exporter, a slowly hydrolyzable ATP analog, such as adenosine 5'-O-(3-thiotriphosphate) (ATPγS) was added to the protein sample just before the grid freezing. By using ATPγS, in the protein sample, the hydrolysis rate of ATP is significantly reduced, and the conformational changes associated with ATP hydrolysis are minimized. This strategy helps to capture the transporter in different conformational states, and some might be more suitable for single-particle cryo-EM analysis. Following the optimizing the uneven particle distribution, 4 datasets [(i)NisT+FC16 with ATPγS (ii)NisT+FC16 without ATPγS (iii)NisT+DDM with ATPγS (iv)NisT+DDM without ATPγS] were collected comprising ~7000 recorded movies in each. One representative micrograph from each of the datasets is shown in Figures 26 and 27.

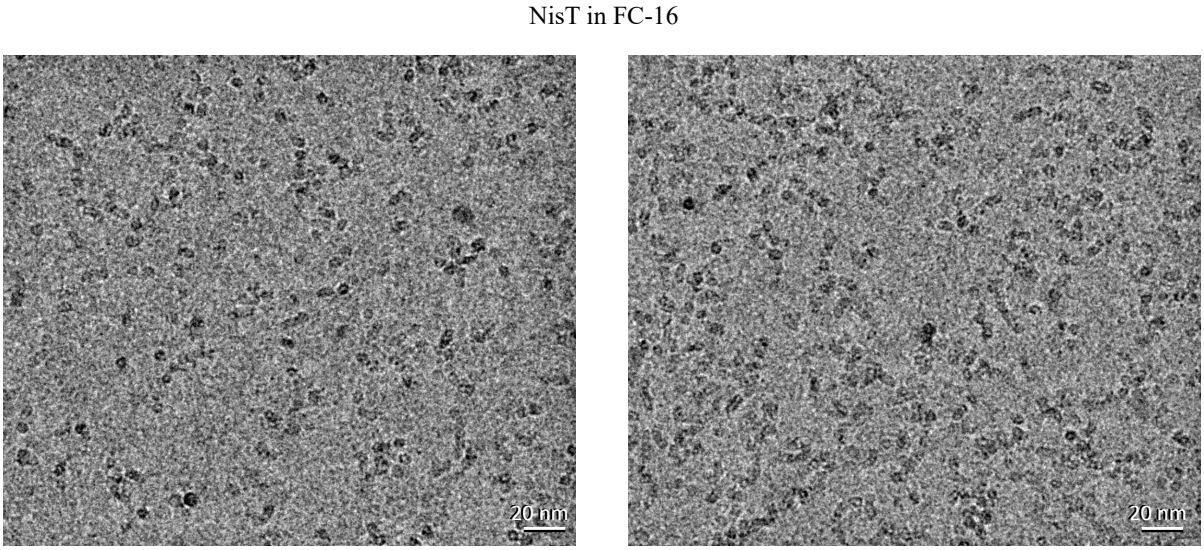

Figure 26. *Single particle cryo-EM micrograph of NisT in FC-16 grid with and without* ATPγS.

NisT in DDM

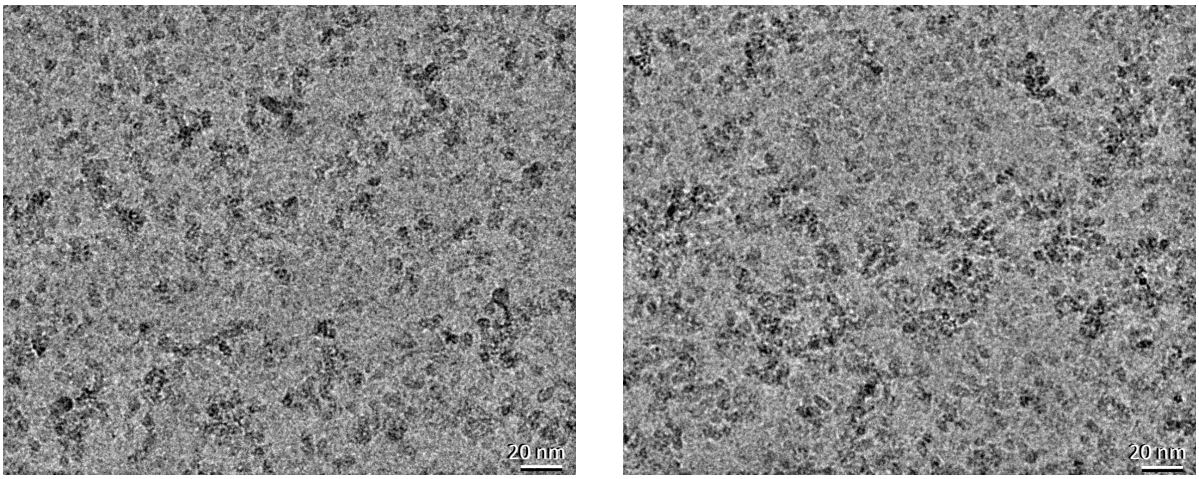

- ATPγS + ATPγS

Figure 27. *Single particle cryo-EM micrograph of NisT in DDM grid with and without* ATPγS.

4.5. NisT cryo-EM data processing:

The typical cryo-EM data processing workflow involves the following steps, i.e., importing the data, motion correction, CTF estimation, particle picking and extraction, 2D classification, 3D reconstruction and result validation[111]. There are many software packages available for carrying out cryo-EM image processing. Some of the commonly used software packages include RELION[94], cryoSPARC[95], SPIDER[112], Frealign[113], EMAN[114], and cisTEM[115]. In our case, both RELION and cryoSPARC software packages were used for image processing.

The images produced by the cryo-EM are two-dimensional projections of the molecule from various angles, which are then processed to reconstruct a three-dimensional model of the molecule. The raw data collected in cryo-EM is typically stored as a series of 2D images in a file format such as MRC or TIFF. These images are often referred to as "frames" or "micrographs" and are usually acquired at a rate of several frames per second.

The first step in cryo-EM data processing is to import these raw data files into software specifically designed for cryo-EM image processing like RELION and cryoSPARC. Once the import step is done, motion correction is essential for obtaining a high-quality 3D

reconstruction of the biological sample. When imaging biological samples using cryo-EM, the samples are embedded in a thin layer of vitrified ice, which is then imaged using an electron microscope. However, during the image collection, the samples may shift due to factors such as stage drift, charging, or beam-induced motion. These movements result in blurred or distorted images, which can reduce the quality of the final 3D reconstruction[116]. Motion correction is a process that corrects these sample movements by aligning the individual micrographs to a common reference. This process involves selecting a reference micrograph and then aligning all the other micrographs to it using cross-correlation or other image alignment algorithms[117]. This ensures that all the micrographs are aligned in the same orientation and position and that any motion-induced blur or distortion is corrected.

After motion correction, Contrast Transfer Function (CTF) estimation is performed. The CTF is a mathematical description of the way in which the electron microscope and the sample interact to produce the recorded image[118]. The CTF estimation is necessary to correct the effects of the CTF on the recorded images and to obtain an accurate 3D reconstruction. The CTF of an electron microscope is affected by various factors such as the energy of the electrons, the defocus of the microscope, and the spherical aberration of the lenses[119]. These factors result in a blurring of the recorded image, which varies with the spatial frequency of the image. This correction is necessary to obtain an accurate 3D reconstruction of the sample. If the CTF is not corrected, the final reconstructed model may suffer from reduced resolution or might contain artifacts and distortions affecting the interpretation of the structure.

Particle picking and extraction are crucial steps for generating a high-quality 3D reconstruction of the macromolecular complex, which involves identifying and extracting individual particles from the raw cryo-EM micrographs. There are several options to perform particle picking and the choice of method often depends on various factors, including the quality of the data, the size and complexity of the particle, and the level of automation desired.

Among these, the common particle picking methods are manual picking, blob picker, template-based picking and deep learning-based picking like TOPAZ[120].

After particle extraction, 2D classification is a recommended step in cryo-EM data processing that helps to improve the quality of the final 3D reconstruction. The goal of 2D classification is to group similar particles based on their 2D projection images, allowing for the removal of poor-quality particles and the selection of high-quality particles for further processing.

For cryo-EM data sets, the researcher often starts with blob picking. In blob picking, the particles are detected as local maxima in the micrographs using blob detection algorithms[121]. These local maxima are essentially blobs in the image that are higher in intensity than their surrounding pixels. The advantage of blob picking is that it can be fast and automated. The algorithms used for blob detection are relatively simple and can be implemented efficiently, which makes it possible to process large datasets quickly. Additionally, blob picking can be effective for detecting particles that are relatively large and well-separated from each other, as the local maxima tend to correspond to particle centers. However, blob picking may not work well for small or low-contrast particles, as these may not generate distinct local maxima[121]. Additionally, blob-picking algorithms may generate false positives if the micrographs contain noise or other features that resemble particle centers. And in our case, the protein size was relatively small, which made it difficult for blob-picking algorithms to distinguish the particles from the background noise or other features in the micrographs, ultimately leading to random/junk particle picking. Random particle picking by the blob picker can result in a particle stack that is noisy and poorly representative of the target structure. In order to avoid random/junk particle picking, different types of parameters can be used in cryo-EM data processing. These parameters can include particle diameter, particle shape, contrast, correlation coefficient, and signal-to-noise ratio. It is important to note that the choice of

parameters will depend on the specific sample and experimental conditions and may require some experimentation to determine the optimal values.

After picking particles from all four NisT datasets using a blob picker in cryoSPARC, 2D class averaging was performed. Unfortunately, the resulting 2D class averages were not promising even after trying different parameters and iterative rounds of classification in the blob-picking job (Figures 28 and 29). Parallel image processing in RELION also displayed similar results as cryoSPARC, and therefore the RELION results are not presented in the thesis.

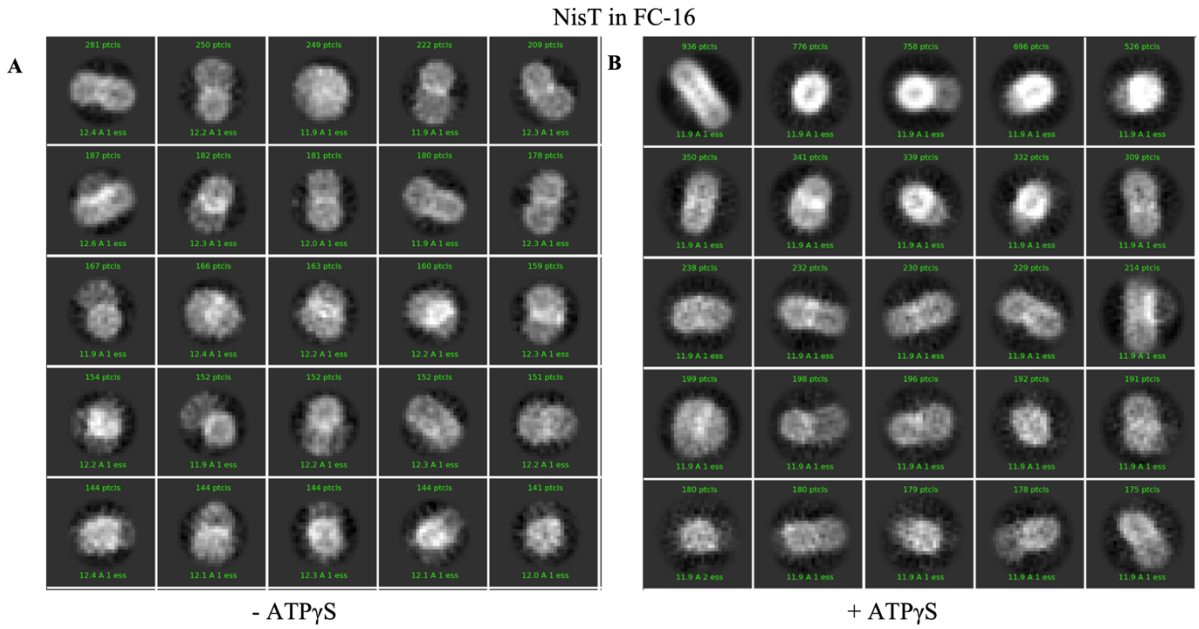

Figure 28. *Representative 2D class averages of NisT in FC-16 particle images using* cryoSPARC's *blob picker (A)without ATPγS (B)with ATPγS*

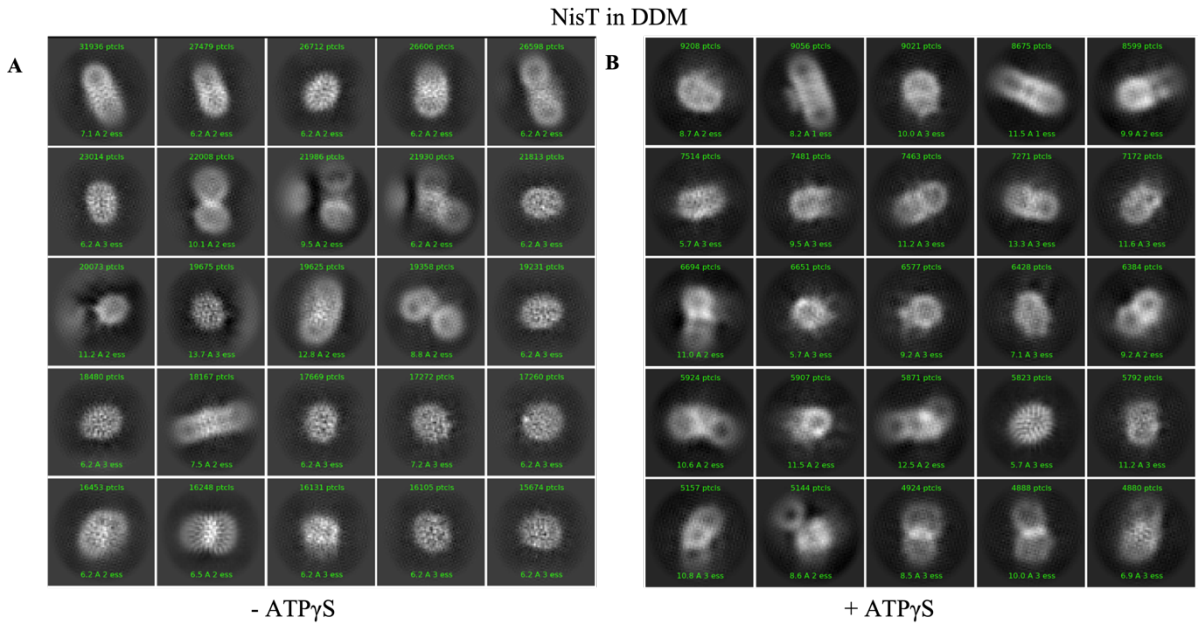

Figure 29. *Representative 2D class averages of NisT in DDM particle images using* cryoSPARC's *blob picker (A)without ATPγS (B)with ATPγS*

Next, we employed the template-based particle-picking method to refine the particle-picking process, for which we have generated an Alphafold model[122,123] of NisT. Since the hydrophobic transmembrane region of NisT is surrounded by a detergent micelle, it is important to generate a template that also contains a detergent micelle. This detergent micelle containing template ensures that the resulting particles are correctly identified and extracted as the detergent micelle give rise to a unique and recognizable shape that can be used to distinguish the NisT transporter particles from other structures in the micrograph. Hence, we incorporated the protein model in a lipid micelle containing FC-16 or DDM detergent using the CHARMM-GUI server[124]. The generated model was then converted into a volume and was imported to cryoSPARC as a template for particle picking (Figure 30). Even in this case, the 2D class averages did not yield classes that resembles an ABC exporter in detergent micelle (Figures 31 and 32).

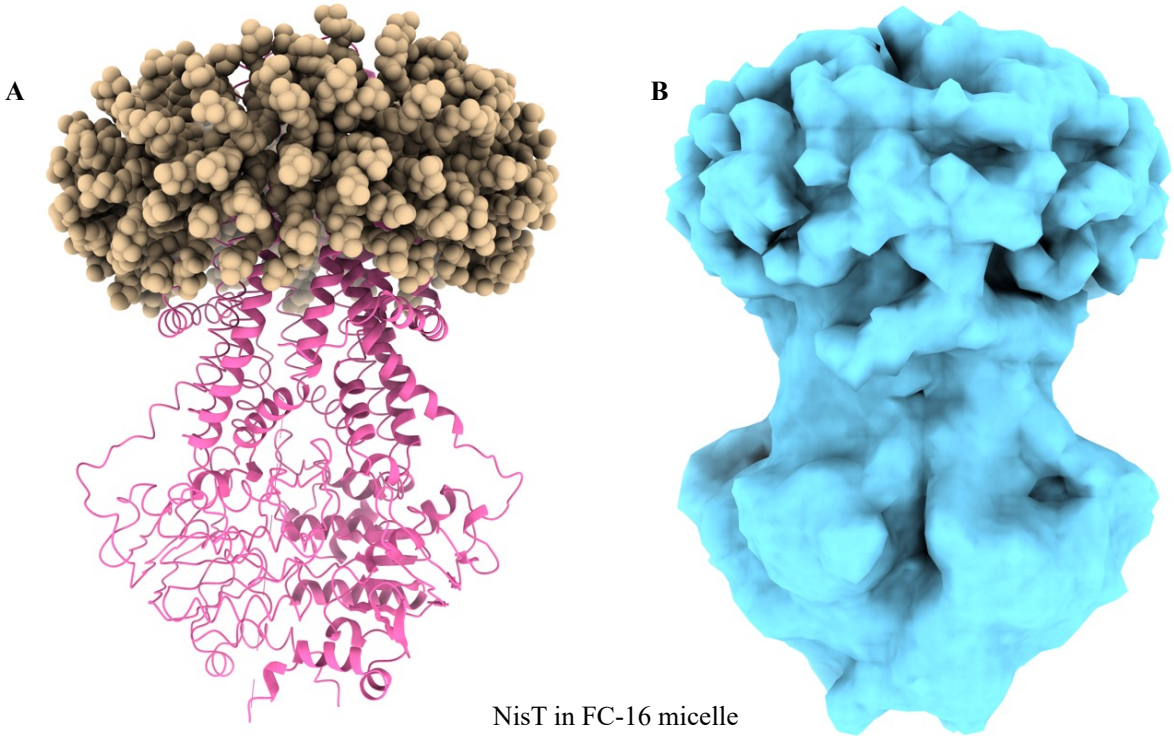

Figure 30. *Template used for template-based particle picking method. (A) NisT alphafold model (in pink) in a lipid micelle (light brown) containing FC-16 detergent (B)Converted volume (in cyan).*

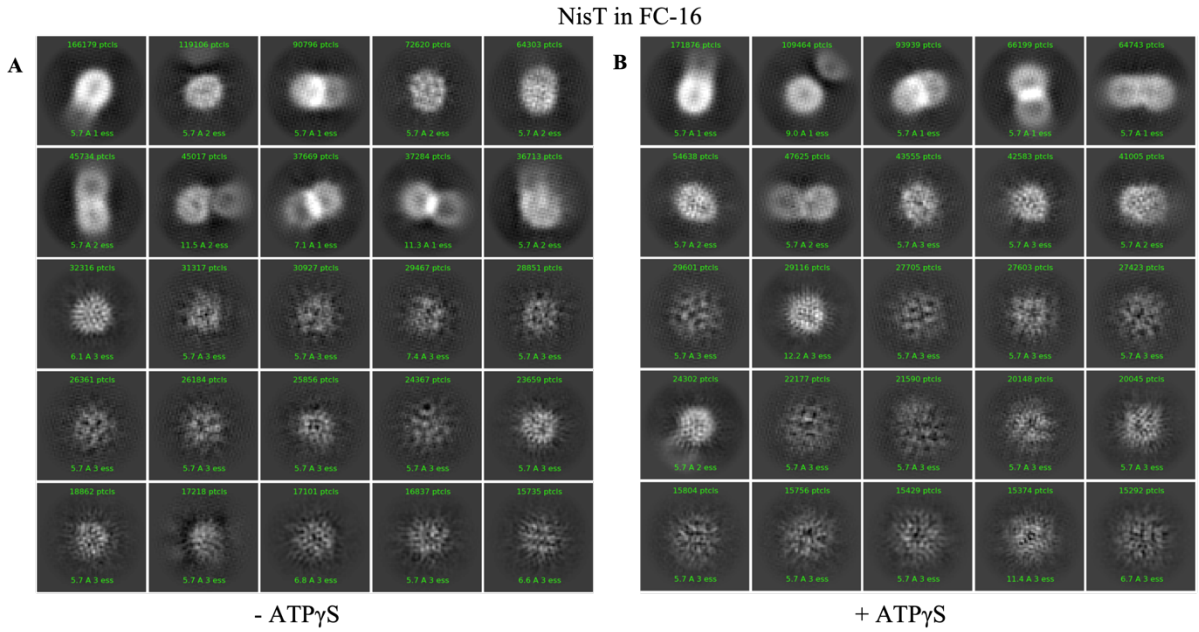

Figure 31. *Representative 2D class averages of NisT in FC-16 particle images using* cryoSPARC's *template picker (A)without ATPγS (B)with ATPγS*

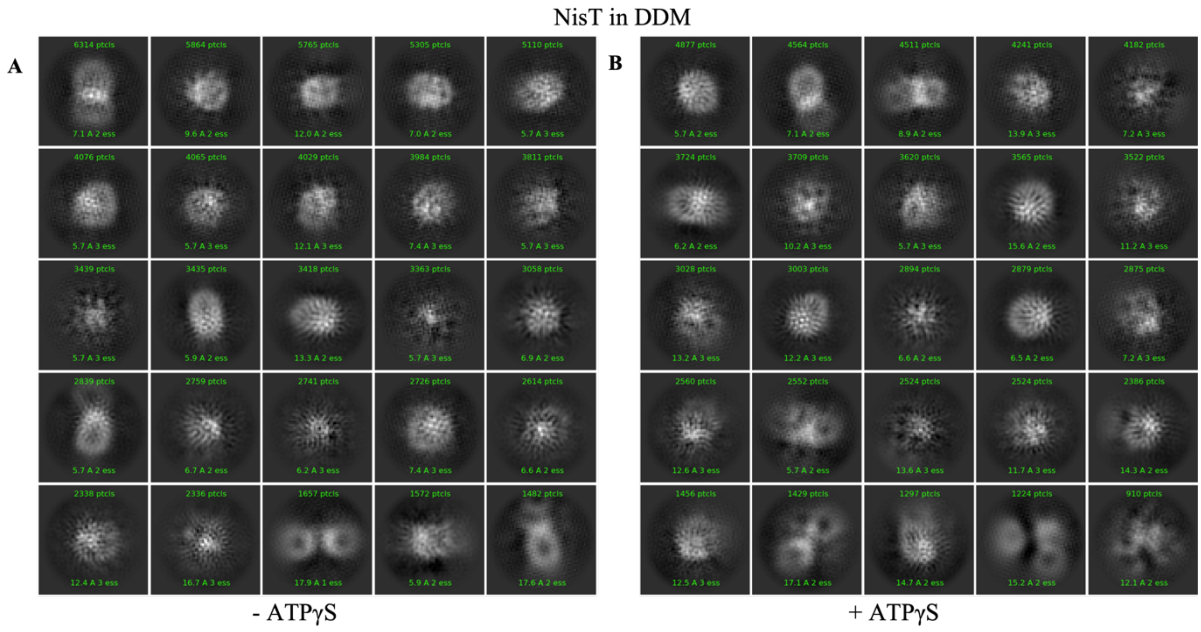

Figure 32. *Representative 2D class averages of NisT in DDM particle images using* cryoSPARC's *template picker (A)without ATPγS (B)with ATPγS*

Blob and template-based particle-picking methods are widely used in cryo-EM data processing, but they can be limited by their reliance on predefined templates or assumptions about the shape and size of the particles. TOPAZ, on the other hand, uses a deep learning-based approach that can adapt to a wide range of particle shapes and sizes, and can potentially improve the accuracy and speed of particle picking[120]. Initially, TOPAZ is trained by multiple rounds in cryoSPARC using a small number of particle stacks as well as a template/volume created previously. Following the training, particle picking was performed again and was followed by 2D class averaging. Here again, the 2D class averages did not yield classes that resemble an ABC exporter in detergent micelle (Figures 33 and 34)

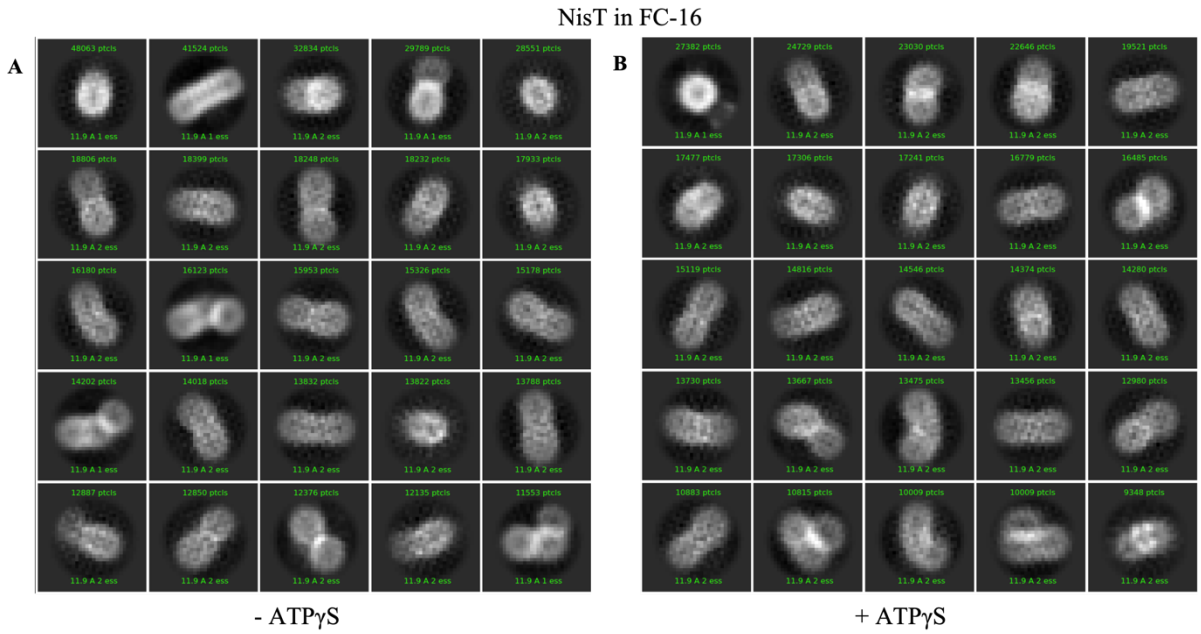

Figure 33. *Representative 2D class averages of NisT in FC-16 particle images using TOPAZ in CryoSparc (A)without ATPγS (B)with ATPγS*

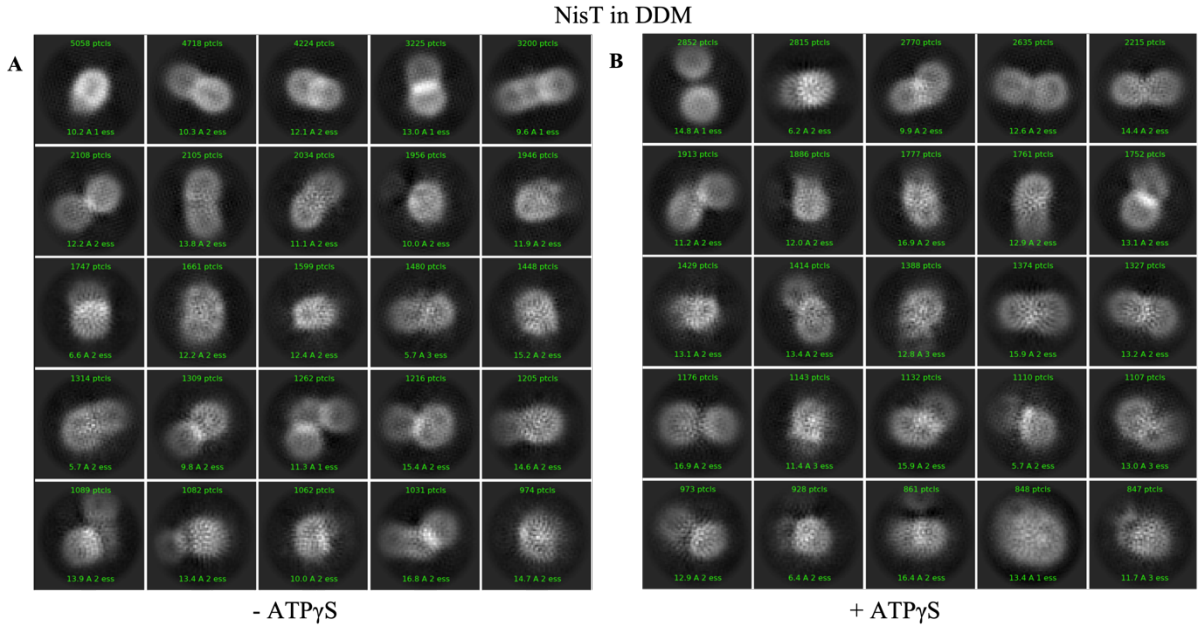

Figure 34. *Representative 2D class averages of NisT in DDM particle images using TOPAZ in CryoSparc (A)without ATPγS (B)with ATPγS*

After trying multiple approaches for particle picking and 2D class averaging, it seemed as if our samples contain only empty detergent micelles, suggesting that the transporter fold was disrupted due to the detergent or there was an excessive amount of empty detergent

micelles present on the grids. Previous studies have suggested that empty detergent micelles often cause problems if they are present in large quantities on the cryo-EM grids[101]. These empty micelles can interfere with the alignment and classification of the real protein particles in the dataset[101]. Empty detergent micelles can also contaminate the cryo-EM grid and cause artifacts in the reconstructed structures. For example, they may introduce additional noise or distortions that can reduce the resolution of the reconstructed images. Detergent micelles can be variable in size and shape, which can make it more difficult to align and classify them accurately[125]. This can lead to lower quality 2D class averages, which in turn can affect the resolution of the final reconstructed structure.

Apart from the structure determination of the NisT transporter, understanding the conformational dynamics of the NisT transporter is crucial for comprehending its function and interactions with other proteins and complexes. Conformational changes play a vital role in protein-protein interactions, which are essential for many biological processes. For example, during the transport cycle, the NisT transporter undergoes a series of conformational changes, including opening and closing of its substrate-binding pocket, as well as structural rearrangements of its transmembrane domains, to facilitate substrate binding and release. By studying these conformational changes in detail, researchers can gain insights into the molecular mechanisms underlying the transport process, which can help in the design of drugs that specifically target the transporter. Furthermore, understanding the conformational changes that occur during protein-protein interactions can also aid in the design of novel therapeutics and drugs that selectively enhance these interactions or disrupt them, depending on the desired outcome.

There are several techniques that can be used to study the conformational dynamics of an ABC transporter even in the absence of high-resolution structural model including Hydrogen-Deuterium Exchange Mass Spectrometry (HDX-MS)[126]. Hence, we have employed

HDX-MS to characterize the conformational dynamics, protein-protein interactions, and ligand binding of NisT transporters.

4.6. HDX-MS Data Collection and Analysis of NisT

In an HDX-MS experiment, optimizing the digestion and liquid chromatography (LC) conditions is crucial to generate a high-quality peptide map. A good peptide map should have high sequence coverage, redundancy, and signal quality[127]. The proteolytic digestion conditions, such as enzyme type, concentration, and digestion time, should be optimized to generate peptides of appropriate length and sequence coverage. The LC conditions, such as column type, gradient, and mobile phase, should also be optimized to ensure good separation and detection of peptides[128]. The quality of the peptide map determines the accuracy and precision of the HDX-MS results, which in turn affects the reliability of the structural information obtained.

Hence, different trap and digestion conditions were examined to get a good peptide map coverage of the NisT reference samples in both FC-16 and DDM detergents (Table 1).

Table 1. *Listed different MS conditions tried for the NisT reference sample.*

Detergent	Sample	MS conditions	PLGS Coverage %	Dynamx coverage with 1 replicate	Dynamx coverage with 2 replicates
F6-16	2 uM NisT	3 min trap 15 C digestion	93.2	47.8	47.1
DDM	2 uM NisT	3 min trap 15 C digestion	91.2	73.6	-
DDM	2 uM NisT	5min trap 15 C digestion	97.3,	90.8	85.3
DDM	2 uM NisT	5min trap 20 C digestion	-	92.0	85.5
F6-16	1 uM	3 min trap 15 C digestion	-	30.3	-
F6-16	1 uM	5 min trap 15 C digestion	-	66.7	-
F6-16	1 uM	5min trap 20 C digestion	-	72.7	-

The sequence coverage map obtained from the NisT/DDM reference sample by LC-MS is 85.3% and 85.5% with 5 minutes of trap/15˚C digestion and 5 minutes of trap/20˚C digestion respectively (Figure 35 and 36).

Figure 35. *The coverage map was recorded for NisT/DDM with* 5 minutes of trap/15˚C digestion.

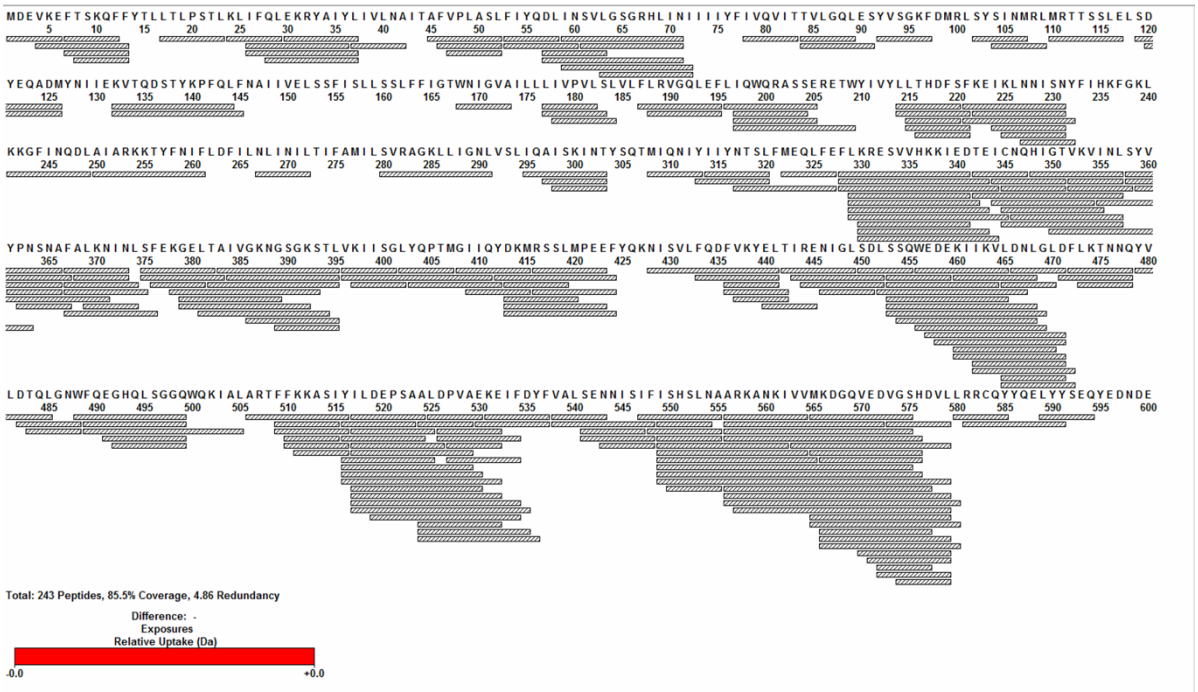

Figure 36. *The coverage map was recorded for NisT/DDM with* 5 minutes of trap/20˚C digestion.

But, in the NisT/FC-16 reference sample, only 47% of the peptide coverage map was obtained (Figure 37), which requires further optimization.

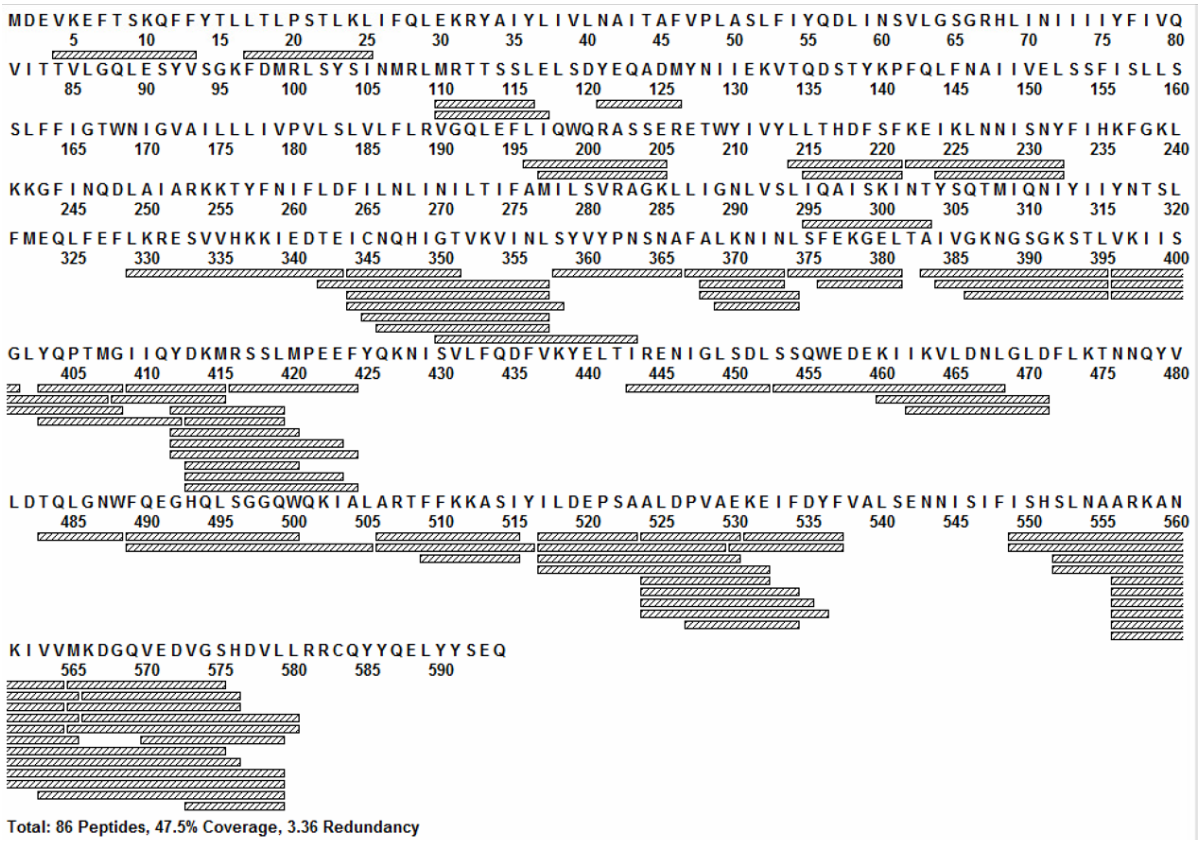

Figure 37. *The coverage map was recorded for NisT/FC-16 with* 3 minutes of trap/15˚C digestion.

Achieving a good peptide map coverage of reference samples is essential for obtaining accurate and reliable HDX-MS data, and careful consideration should be given to the choice of enzyme and digestion conditions to ensure optimal results. In our case, NisT in the presence of DDM gave a good sequence coverage of 85%, indicating that a large portion of the NisT sequence was identified and analyzed by mass spectrometry. However, it is not a complete sequence coverage, and there may be some regions of the protein that cannot be analyzed due to the limitations of the LC-MS method, or the digestion conditions used. However, in the case of the NisT in the presence of FC-16 reference sample, only 47% of the peptide coverage map was obtained. This low percentage of sequence coverage suggests that further optimization of the experimental conditions is necessary to improve the digestion and peptide recovery.

5. Discussion:

Membrane proteins are essential for many biological processes and are targets for numerous pharmaceuticals[129]. However, the study of these proteins is challenging, mainly due to their hydrophobic nature and the difficulties associated with extracting them from the membrane. The optimization of the membrane protein expression and purification is a challenging process but necessary to obtain a high yield of the protein for biochemical or structural analysis. When attempting to solubilize and stabilize membrane proteins, it is vital to carefully select the appropriate detergent. Because different detergents have different affinities for different parts of the protein, the wrong detergent can result in protein denaturation, aggregation or loss of its functionality[17]. Several factors should be considered when selecting a detergent suitable for solubilizing and stabilizing membrane proteins[130]. The first factor is the size of the detergent micelle. It is necessary to choose a detergent that can form small micelles that can efficiently solubilize the protein, but not so small that it cannot protect the protein's hydrophobic regions. The second factor to consider is the structure of the protein. Some detergents are better suited for certain protein structures, such as alpha-helical or beta-barrel proteins[101]. The third factor to consider is the detergent properties. The hydrophobic and hydrophilic properties of the detergent should match the properties of the protein being studied. The choice of detergent will depend on the specific protein and the desired experimental conditions. Therefore, it is necessary to select a detergent that is best suited for the specific structure of the protein under investigation[130].

In the case of NisT, extensive optimization of the purification process was conducted by screening a wide range of detergents to identify the most effective ones. In previous studies as well as our study, NisT was found to be active and stable in FC-16 detergent, suggesting that FC-16 detergent is suitable for solubilizing and stabilizing the protein during the purification process[5]. However, FC-16 is not always the preferred detergent for the

solubilization of membrane proteins due to its harsh nature. The fact that NisT is also stable and active in DDM, a commonly used non-ionic detergent, presents an alternative and milder approach for solubilization that will be more flexible for downstream applications. To further validate the stability and activity of NisT, we performed the ATPase assay of NisT in both DDM and FC-16, suggesting that NisT is functional and able to catalyze the hydrolysis of ATP. This ATPase activity assay serves as an important validation suggesting that the purified protein is indeed properly folded. In the future, it is important to record the ATPase activity of NisT in the presence/absence of NisA, NisB, and NisC to determine if protein-protein interactions influence the ATP hydrolysis rate.

After successfully validating NisT activity in both DDM and FC-16 detergents, we initiated a structural study using cryo-EM to gain structural insights into its molecular architecture. However, during the image processing, we encountered difficulties to obtain high-quality 2D class averages from the cryo-EM datasets. To address these issues, we tested different strategies in efforts to improve the particle selection and downstream 2D class averages including template-based particle picking and TOPAZ picking as alternative methods for particle selection.

Template-based particle picking involves using a high-resolution reference structure to search for and extract particles from the micrographs[131]. Template-based particle picking is a widely used method in cryo-EM for identifying and extracting particles from micrographs. While this approach can be effective, it also has several limitations[132]. One of the limitations of template-based particle picking in cryo-EM is the potential for introducing bias in the selection of particles. The use of a reference structure can introduce a degree of subjectivity into the particle-picking process, as the choice of the reference can influence the particles that are selected. This can be especially problematic if the reference structure is incomplete or

incorrect and may lead to the selection of only a subset of particles, potentially skewing the final results. Despite the potential of bias introduction, template-based particle picking in cryo-EM remains a valuable method as it can be effective in identifying and extracting particles from micrographs, particularly when a high-resolution reference structure is available. One advantage of template-based particle picking is that it can be more accurate than other methods, particularly when the reference structure is not well-resolved and matches the particles in the micrographs. This can result in higher quality 2D class averages and a more complete dataset, leading to a more accurate 3D structure. Finally, template-based particle picking can be combined with other methods, such as ab-initio reconstruction or focused classification, to increase the diversity of particle populations and reduce potential biases. By using multiple references or combining template-based particle picking with other methods, researchers can obtain more accurate and complete datasets, and increase the resolution and accuracy of the final 3D structure. Hence, we generated a model of NisT and detergents complex using Alphafold[122,123] and CHARMM-GUI[124] and used it as a template for particle picking. While this approach helped in identifying particles, the quality of the 2D class averages remained suboptimal.

Furthermore, when traditional methods like blob and template-based picking failed to produce satisfactory 2D class averages, we explored TOPAZ for particle picking. TOPAZ is an automated particle-picking tool that uses a deep learning-based approach to identify and extract particles from cryo-EM micrographs[120]. One of the advantages of TOPAZ is its high speed and accuracy. It can quickly identify particles in micrographs, even in noisy or low-contrast images, and accurately extract them for further processing. Another advantage of TOPAZ is its ability to detect and remove false positives, which can be particularly important when dealing with complex datasets or noisy micrographs[120]. By reducing the number of false

positives, TOPAZ can produce more accurate and reliable results, leading to a higher-quality 3D structure. However, TOPAZ also has its own limitations. It requires a large amount of training data to achieve high accuracy, and the quality of the dataset can depend on the quality of the training data. Additionally, it may not perform as well on samples with significant conformational heterogeneity or low particle density. Despite its limitations, we have utilized TOPAZ. However, even after multiple rounds of training in cryoSPARC using a small number of particle stacks as well as a template/volume created previously, the collected cryo-EM datasets resulted in suboptimal 2D class averages.

After all these rigorous optimizations in the cryo-EM image processing pipeline, we suspect that the problem might be with the sample itself. One of the reasons could be the presence of a high concentration of empty detergent micelles on the cryo-EM grids. During concentrating the protein, not all detergent micelles pass through the spin concentrator even if the molecular cutoff is higher than the detergent micelle size. There could be different reasons, sometimes the detergent micelles can adhere to the membrane of a spin concentrator during the concentration process, especially if the detergent concentration is too high. Another reason could be that the detergent micelles have become too large or too stable to be disrupted by the centrifugal force applied during the concentration process. This can occur if the detergent concentration is too high or if the detergent has formed large aggregates or micelles due to factors such as pH, temperature, or ionic strength. Regardless of the cause, the presence of empty detergent micelles on cryo-EM grids represents a real problem as they can interfere with the visualization of the protein of interest. The empty micelles can scatter electrons and create noise in the cryo-EM images, which can make it difficult to obtain high-quality reconstructions of the protein structure. To mitigate this issue, membrane mimetic systems such peptidisc[103], nanodisc[102], saposinA[104], SMALPS[105] and liposomes[106] can be used.

Hence, here we have used peptidisc to reconstitute NisT, where the on-column peptidisc reconstitution showed a NisT/peptidisc complex population on the SEC chromatogram, suggesting the NisT dimer is properly folded and stable. An ATPase assay of the peptidic-reconstituted NisT is required to further confirm its activity. Also reconstituting NisT with nanodisc would be a desirable option to continue and explore as it has several benefits in comparison to detergent micelles. Incorporation of NisT into nanosidcs can help to stabilize the protein complex and prevent its denaturation or aggregation as it provides a more natural environment for the protein complex, where it is surrounded by a lipid bilayer similar to those of biological membranes. According to our challenges in determining the high-resolution structure of NisT in detergents, both peptidiscs and nanodiscs serve as promising alternatives. Moreover, peptidiscs or nanodiscs have a lower tendency to disrupt protein-protein interactions, they can be important for determining the structure of NisT[103].

In addition to determining the structure of the NisT transporter, we employed HDX-MS to better understand the conformational dynamics of NisT. Peptide coverage determination is an important step prior to a successful HDX-MS experiment. Peptide coverage refers to the proportion of the protein sequence that is covered by the peptides generated during HDX-MS sample preparation. The higher coverage of the protein sequence, the more comprehensive the HDX-MS analysis will be. In our case, NisT in the presence of DDM gave an 85% sequence coverage map, indicating that a large portion of the NisT protein sequence can be identified and analyzed by mass spectrometry. But, for NisT in FC-16 reference sample, only 47% of the peptide coverage map was obtained. There are several possible reasons for the lower sequence coverage obtained with the NisT in FC-16 sample. First, the different detergent used in the sample preparation (FC-16 instead of DDM) may have altered the protein structure and/or affected the enzymatic digestion, leading to reduced peptide recovery. Second, the digestion conditions used for the NisT in FC-16 sample may not have been optimized for this particular

sample, and alternative digestion conditions or enzymes should be tested to improve the peptide coverage. These attempts should include digestion conditions optimization, using different proteases or enzymes, or adjusting the LC-MS parameters. Additionally, the use of alternative mass spectrometry techniques such as top-down or middle-down fragmentation may provide a more comprehensive analysis of intact protein structures and help to fill in any gaps in the sequence coverage. Furthermore, HDX-MS can be used to investigate the conformational dynamics of NisT upon binging NisA and other interacting binding partners like NisB and NisC.

6. Final conclusion and summary:

Biosynthetic enzymes are powerful tools for producing structurally complex molecules of biomedical relevance using renewable resources. They are capable of assembling complex molecules from simpler building blocks, and they can do this with high efficiency and selectivity. This makes them powerful tools for producing structurally complex molecules, such as pharmaceuticals, using renewable resources. One example of biosynthetic enzymes in action is the production of the Nisin. Nisin is a small peptide antibiotic that is produced by the bacterium *Lactococcus lactis*, through a process known as ribosomally synthesized and post-translationally modified peptides (RiPPs). It is used as a food preservative and has potential therapeutic applications as well. The biosynthetic pathway for Nisin involves the action of several enzymes, including NisB, NisC, NisP, and NisT. Investigation into the role of biophysical processes in the nisin biosynthetic pathway can provide a blueprint for the investigation of other RiPP biosynthetic pathways leveraging similar cryoEM and MS-based quantitative approaches.

The research presented in this thesis represents a significant step toward a comprehensive understanding of the structure and function of the NisT transporter protein. The successful optimization of protein expression and purification allowed for the acquisition of high-quality protein samples, which were then used for functional and structural analyses. The ATPase assay demonstrated that the protein is active while the initial cryo-EM structural studies presented revealed that further optimization is still required to obtain a high-resolution structure. This observation highlights the complexity of the NisT and the challenges associated with membrane proteins characterization using cryo- EM. Ultimately, a more detailed understanding of the structure of the NisT transporter protein could provide insights into its function, which could have important implications in the development of novel antimicrobial agents.

7. Reference:

1. Rees DC, Johnson E, Lewinson O. ABC transporters: the power to change. Nat Rev Mol Cell Biol 2009;10(3):218-27, doi:10.1038/nrm2646
2. van der Donk WA, Nair SK. Structure and mechanism of lanthipeptide biosynthetic enzymes. Curr Opin Struct Biol 2014;29(58-66, doi:10.1016/j.sbi.2014.09.006
3. Cao L, Do T, Link AJ. Mechanisms of action of ribosomally synthesized and posttranslationally modified peptides (RiPPs). J Ind Microbiol Biotechnol 2021;48(3-4), doi:10.1093/jimb/kuab005
4. Hudson GA, Mitchell DA. RiPP antibiotics: biosynthesis and engineering potential. Curr Opin Microbiol 2018;45(61-69, doi:10.1016/j.mib.2018.02.010
5. Lagedroste M, Reiners J, Smits SHJ, et al. Impact of the nisin modification machinery on the transport kinetics of NisT. Scientific Reports 2020;10(1):12295, doi:10.1038/s41598-020-69225-2
6. Repka LM, Chekan JR, Nair SK, et al. Mechanistic Understanding of Lanthipeptide Biosynthetic Enzymes. Chemical Reviews 2017;117(8):5457-5520, doi:10.1021/acs.chemrev.6b00591
7. Prestinaci F, Pezzotti P, Pantosti A. Antimicrobial resistance: a global multifaceted phenomenon. Pathog Glob Health 2015;109(7):309-18, doi:10.1179/2047773215y.0000000030
8. Luo GG, Gao SJ. Global health concerns stirred by emerging viral infections. J Med Virol 2020;92(4):399-400, doi:10.1002/jmv.25683
9. Murray CJL, Ikuta KS, Sharara F, et al. Global burden of bacterial antimicrobial resistance in 2019: a systematic analysis. The Lancet 2022;399(10325):629-655, doi:10.1016/S0140-6736(21)02724-0
10. Neely AN, Holder IA. Antimicrobial resistance. Burns 1999;25(1):17-24
11. O'Neill J. Tackling drug-resistant infections globally: final report and recommendations. 2016;
12. Al-Tawfiq JA, Momattin H, Al-Ali AY, et al. Antibiotics in the pipeline: a literature review (2017-2020). Infection 2022;50(3):553-564, doi:10.1007/s15010-021-01709-3
13. Aminov RI. A brief history of the antibiotic era: lessons learned and challenges for the future. Front Microbiol 2010;1(134, doi:10.3389/fmicb.2010.00134
14. Llor C, Bjerrum L. Antimicrobial resistance: risk associated with antibiotic overuse and initiatives to reduce the problem. Ther Adv Drug Saf 2014;5(6):229-41, doi:10.1177/2042098614554919
15. Munita JM, Arias CA. Mechanisms of Antibiotic Resistance. Microbiol Spectr 2016;4(2), doi:10.1128/microbiolspec.VMBF-0016-2015
16. Reygaert WC. An overview of the antimicrobial resistance mechanisms of bacteria. AIMS Microbiol 2018;4(3):482-501, doi:10.3934/microbiol.2018.3.482
17. Lv L, Wan M, Wang C, et al. Emergence of a Plasmid-Encoded Resistance-Nodulation-Division Efflux Pump Conferring Resistance to Multiple Drugs, Including Tigecycline, in Klebsiella pneumoniae. mBio 2020;11(2), doi:10.1128/mBio.02930-19
18. Abdi SN, Ghotaslou R, Ganbarov K, et al. Acinetobacter baumannii Efflux Pumps and Antibiotic Resistance. Infect Drug Resist 2020;13(423-434, doi:10.2147/idr.S228089
19. Webber MA, Piddock LJ. The importance of efflux pumps in bacterial antibiotic resistance. J Antimicrob Chemother 2003;51(1):9-11, doi:10.1093/jac/dkg050
20. Kornelsen V, Kumar A. Update on Multidrug Resistance Efflux Pumps in Acinetobacter spp. Antimicrobial Agents and Chemotherapy 2021;65(7):e00514-21, doi:doi:10.1128/AAC.00514-21

21. Borges-Walmsley MI, McKeegan KS, Walmsley AR. Structure and function of efflux pumps that confer resistance to drugs. Biochem J 2003;376(Pt 2):313-38, doi:10.1042/bj20020957
22. Sharma A, Gupta VK, Pathania R. Efflux pump inhibitors for bacterial pathogens: From bench to bedside. Indian J Med Res 2019;149(2):129-145, doi:10.4103/ijmr.IJMR_2079_17
23. Schenone M, Dančík V, Wagner BK, et al. Target identification and mechanism of action in chemical biology and drug discovery. Nat Chem Biol 2013;9(4):232-40, doi:10.1038/nchembio.1199
24. Arthur M, Courvalin P. Genetics and mechanisms of glycopeptide resistance in enterococci. Antimicrobial Agents and Chemotherapy 1993;37(8):1563-1571, doi:doi:10.1128/AAC.37.8.1563
25. Matsuo M, Cui L, Kim J, et al. Comprehensive identification of mutations responsible for heterogeneous vancomycin-intermediate Staphylococcus aureus (hVISA)-to-VISA conversion in laboratory-generated VISA strains derived from hVISA clinical strain Mu3. Antimicrob Agents Chemother 2013;57(12):5843-53, doi:10.1128/aac.00425-13
26. Wilson DN. The ABC of Ribosome-Related Antibiotic Resistance. mBio 2016;7(3):e00598-16, doi:doi:10.1128/mBio.00598-16
27. Egorov AM, Ulyashova MM, Rubtsova MY. Bacterial Enzymes and Antibiotic Resistance. Acta Naturae 2018;10(4):33-48
28. Abdollahi M, Mostafalou S. Chloramphenicol. In: Encyclopedia of Toxicology (Third Edition). (Wexler P. ed.) Academic Press: Oxford; 2014; pp. 837-840.
29. Shaw WV. Chloramphenicol acetyltransferase: enzymology and molecular biology. CRC Crit Rev Biochem 1983;14(1):1-46, doi:10.3109/10409238309102789
30. Tooke CL, Hinchliffe P, Bragginton EC, et al. β-Lactamases and β-Lactamase Inhibitors in the 21st Century. J Mol Biol 2019;431(18):3472-3500, doi:10.1016/j.jmb.2019.04.002
31. Bush K. Bench-to-bedside review: The role of β-lactamases in antibiotic-resistant Gram-negative infections. Critical Care 2010;14(3):224, doi:10.1186/cc8892
32. Mingeot-Leclercq MP, Glupczynski Y, Tulkens PM. Aminoglycosides: activity and resistance. Antimicrob Agents Chemother 1999;43(4):727-37, doi:10.1128/aac.43.4.727
33. Nicholson JR, Sommer B. The research domain criteria framework in drug discovery for neuropsychiatric diseases: focus on negative valence. Brain and Neuroscience Advances 2018;2(2398212818804030, doi:10.1177/2398212818804030
34. Ferguson LB, Harris RA, Mayfield RD. From gene networks to drugs: systems pharmacology approaches for AUD. Psychopharmacology 2018;235(6):1635-1662, doi:10.1007/s00213-018-4855-2
35. Dutescu IA, Hillier SA. Encouraging the Development of New Antibiotics: Are Financial Incentives the Right Way Forward? A Systematic Review and Case Study. Infect Drug Resist 2021;14(415-434, doi:10.2147/idr.S287792
36. Szymański P, Markowicz M, Mikiciuk-Olasik E. Adaptation of high-throughput screening in drug discovery-toxicological screening tests. Int J Mol Sci 2012;13(1):427-52, doi:10.3390/ijms13010427
37. Rao C, Huisman DH, Vieira HM, et al. A Gene Expression High-Throughput Screen (GE-HTS) for Coordinated Detection of Functionally Similar Effectors in Cancer. Cancers (Basel) 2020;12(11), doi:10.3390/cancers12113143
38. Paricharak S, Méndez-Lucio O, Chavan Ravindranath A, et al. Data-driven approaches used for compound library design, hit triage and bioactivity modeling in high-throughput screening. Brief Bioinform 2018;19(2):277-285, doi:10.1093/bib/bbw105
39. Hughes JP, Rees S, Kalindjian SB, et al. Principles of early drug discovery. Br J Pharmacol 2011;162(6):1239-49, doi:10.1111/j.1476-5381.2010.01127.x

40. Sliwoski G, Kothiwale S, Meiler J, et al. Computational methods in drug discovery. Pharmacol Rev 2014;66(1):334-95, doi:10.1124/pr.112.007336
41. Verma S, Prabhakar YS. Target based drug design - a reality in virtual sphere. Curr Med Chem 2015;22(13):1603-30, doi:10.2174/0929867322666150209151209
42. Moffat JG, Vincent F, Lee JA, et al. Opportunities and challenges in phenotypic drug discovery: an industry perspective. Nature Reviews Drug Discovery 2017;16(8):531-543, doi:10.1038/nrd.2017.111
43. Berg EL. The future of phenotypic drug discovery. Cell Chemical Biology 2021;28(3):424-430, doi:https://doi.org/10.1016/j.chembiol.2021.01.010
44. Moellering RE, Cravatt BF. How chemoproteomics can enable drug discovery and development. Chem Biol 2012;19(1):11-22, doi:10.1016/j.chembiol.2012.01.001
45. Frediansyah A, Sofyantoro F, Alhumaid S, et al. Microbial Natural Products with Antiviral Activities, Including Anti-SARS-CoV-2: A Review. Molecules 2022;27(13), doi:10.3390/molecules27134305
46. Anarat-Cappillino G, Sattely ES. The chemical logic of plant natural product biosynthesis. Curr Opin Plant Biol 2014;19(51-8, doi:10.1016/j.pbi.2014.03.007
47. Hubrich F, Bösch NM, Chepkirui C, et al. Ribosomally derived lipopeptides containing distinct fatty acyl moieties. Proceedings of the National Academy of Sciences 2022;119(3):e2113120119, doi:doi:10.1073/pnas.2113120119
48. Felnagle EA, Jackson EE, Chan YA, et al. Nonribosomal peptide synthetases involved in the production of medically relevant natural products. Mol Pharm 2008;5(2):191-211, doi:10.1021/mp700137g
49. Shin JM, Gwak JW, Kamarajan P, et al. Biomedical applications of nisin. J Appl Microbiol 2016;120(6):1449-65, doi:10.1111/jam.13033
50. Salle AJ, Jann GJ. Subtilin-An Antibiotic Produced by Bacillus subtilis. I. Action on Various Organisms. Proceedings of the Society for Experimental Biology and Medicine 1945;60(1):60-64, doi:10.3181/00379727-60-15091
51. de Veer SJ, Kan M-W, Craik DJ. Cyclotides: From Structure to Function. Chemical Reviews 2019;119(24):12375-12421, doi:10.1021/acs.chemrev.9b00402
52. Buchman GW, Banerjee S, Hansen JN. Structure, expression, and evolution of a gene encoding the precursor of nisin, a small protein antibiotic. J Biol Chem 1988;263(31):16260-6
53. Darbandi A, Asadi A, Mahdizade Ari M, et al. Bacteriocins: Properties and potential use as antimicrobials. Journal of Clinical Laboratory Analysis 2022;36(1):e24093, doi:https://doi.org/10.1002/jcla.24093
54. Dickman R, Mitchell SA, Figueiredo AM, et al. Molecular Recognition of Lipid II by Lantibiotics: Synthesis and Conformational Studies of Analogues of Nisin and Mutacin Rings A and B. J Org Chem 2019;84(18):11493-11512, doi:10.1021/acs.joc.9b01253
55. Berger EA, Heppel LA. Different mechanisms of energy coupling for the shock-sensitive and shock-resistant amino acid permeases of Escherichia coli. J Biol Chem 1974;249(24):7747-55
56. Tarling EJ, de Aguiar Vallim TQ, Edwards PA. Role of ABC transporters in lipid transport and human disease. Trends Endocrinol Metab 2013;24(7):342-50, doi:10.1016/j.tem.2013.01.006
57. Remy E, Duque P. Beyond cellular detoxification: a plethora of physiological roles for MDR transporter homologs in plants. Frontiers in Physiology 2014;5(doi:10.3389/fphys.2014.00201
58. Moussatova A, Kandt C, O'Mara ML, et al. ATP-binding cassette transporters in Escherichia coli. Biochimica et Biophysica Acta (BBA) - Biomembranes 2008;1778(9):1757-1771, doi:https://doi.org/10.1016/j.bbamem.2008.06.009

59. Liu X. ABC Family Transporters. Adv Exp Med Biol 2019;1141(13-100, doi:10.1007/978-981-13-7647-4_2
60. Moore JM, Bell EL, Hughes RO, et al. ABC transporters: human disease and pharmacotherapeutic potential. Trends in Molecular Medicine 2023;29(2):152-172, doi:10.1016/j.molmed.2022.11.001
61. Guo X, Chen X, Weber IT, et al. Molecular basis for differential nucleotide binding of the nucleotide-binding domain of ABC-transporter CvaB. Biochemistry 2006;45(48):14473-80, doi:10.1021/bi061506i
62. Davidson AL, Dassa E, Orelle C, et al. Structure, function, and evolution of bacterial ATP-binding cassette systems. Microbiol Mol Biol Rev 2008;72(2):317-64, table of contents, doi:10.1128/mmbr.00031-07
63. Stratford FL, Ramjeesingh M, Cheung JC, et al. The Walker B motif of the second nucleotide-binding domain (NBD2) of CFTR plays a key role in ATPase activity by the NBD1-NBD2 heterodimer. Biochem J 2007;401(2):581-6, doi:10.1042/bj20060968
64. Smith PC, Karpowich N, Millen L, et al. ATP binding to the motor domain from an ABC transporter drives formation of a nucleotide sandwich dimer. Mol Cell 2002;10(1):139-49, doi:10.1016/s1097-2765(02)00576-2
65. Shin M, Puchades C, Asmita A, et al. Structural basis for distinct operational modes and protease activation in AAA+ protease Lon. Sci Adv 2020;6(21):eaba8404, doi:10.1126/sciadv.aba8404
66. Silverton L, Dean M, Moitra K. Variation and evolution of the ABC transporter genes ABCB1, ABCC1, ABCG2, ABCG5 and ABCG8: implication for pharmacogenetics and disease. Drug Metabol Drug Interact 2011;26(4):169-79, doi:10.1515/dmdi.2011.027
67. Locher KP, Lee AT, Rees DC. The E. coli BtuCD structure: a framework for ABC transporter architecture and mechanism. Science 2002;296(5570):1091-8, doi:10.1126/science.1071142
68. Hollenstein K, Frei DC, Locher KP. Structure of an ABC transporter in complex with its binding protein. Nature 2007;446(7132):213-6, doi:10.1038/nature05626
69. El-Awady R, Saleh E, Hashim A, et al. The Role of Eukaryotic and Prokaryotic ABC Transporter Family in Failure of Chemotherapy. Frontiers in Pharmacology 2017;7(doi:10.3389/fphar.2016.00535
70. Lewinson O, Lee AT, Locher KP, et al. A distinct mechanism for the ABC transporter BtuCD-BtuF revealed by the dynamics of complex formation. Nat Struct Mol Biol 2010;17(3):332-8, doi:10.1038/nsmb.1770
71. Lewinson O, Livnat-Levanon N. Mechanism of Action of ABC Importers: Conservation, Divergence, and Physiological Adaptations. Journal of Molecular Biology 2017;429(5):606-619, doi:https://doi.org/10.1016/j.jmb.2017.01.010
72. Lewinson O, Orelle C, Seeger MA. Structures of ABC transporters: handle with care. FEBS Letters 2020;594(23):3799-3814, doi:https://doi.org/10.1002/1873-3468.13966
73. Qasem-Abdullah H, Perach M, Livnat-Levanon N, et al. ATP binding and hydrolysis disrupt the high-affinity interaction between the heme ABC transporter HmuUV and its cognate substrate-binding protein. J Biol Chem 2017;292(35):14617-14624, doi:10.1074/jbc.M117.779975
74. Hu Y, Rech S, Gunsalus RP, et al. Crystal structure of the molybdate binding protein ModA. Nat Struct Biol 1997;4(9):703-7, doi:10.1038/nsb0997-703
75. Oldham ML, Chen J. Crystal Structure of the Maltose Transporter in a Pretranslocation Intermediate State. Science 2011;332(6034):1202-1205, doi:doi:10.1126/science.1200767
76. Nguyen PT, Lai JY, Kaiser JT, et al. Structures of the Neisseria meningitides methionine-binding protein MetQ in substrate-free form and bound to l- and d-methionine isomers. Protein Sci 2019;28(10):1750-1757, doi:10.1002/pro.3694

77. Chen J. Molecular mechanism of the Escherichia coli maltose transporter. Curr Opin Struct Biol 2013;23(4):492-8, doi:10.1016/j.sbi.2013.03.011
78. Boos W, Shuman H. Maltose/maltodextrin system of Escherichia coli: transport, metabolism, and regulation. Microbiol Mol Biol Rev 1998;62(1):204-29, doi:10.1128/mmbr.62.1.204-229.1998
79. Oldham ML, Khare D, Quiocho FA, et al. Crystal structure of a catalytic intermediate of the maltose transporter. Nature 2007;450(7169):515-521, doi:10.1038/nature06264
80. Rice AJ, Park A, Pinkett HW. Diversity in ABC transporters: Type I, II and III importers. Critical Reviews in Biochemistry and Molecular Biology 2014;49(5):426-437, doi:10.3109/10409238.2014.953626
81. Choi CC, Ford RC. ATP binding cassette importers in eukaryotic organisms. Biological Reviews 2021;96(4):1318-1330, doi:https://doi.org/10.1111/brv.12702
82. Korkhov VM, Mireku SA, Locher KP. Structure of AMP-PNP-bound vitamin B12 transporter BtuCD–F. Nature 2012;490(7420):367-372, doi:10.1038/nature11442
83. Sharom FJ. The P-glycoprotein multidrug transporter. Essays Biochem 2011;50(1):161-78, doi:10.1042/bse0500161
84. Ward AB, Szewczyk P, Grimard V, et al. Structures of P-glycoprotein reveal its conformational flexibility and an epitope on the nucleotide-binding domain. Proceedings of the National Academy of Sciences 2013;110(33):13386-13391, doi:doi:10.1073/pnas.1309275110
85. Johnson ZL, Chen J. Structural Basis of Substrate Recognition by the Multidrug Resistance Protein MRP1. Cell 2017;168(6):1075-1085.e9, doi:https://doi.org/10.1016/j.cell.2017.01.041
86. Rosenberg MF, Mao Q, Holzenburg A, et al. The Structure of the Multidrug Resistance Protein 1 (MRP1/ABCC1): CRYSTALLIZATION AND SINGLE-PARTICLE ANALYSIS*. Journal of Biological Chemistry 2001;276(19):16076-16082, doi:https://doi.org/10.1074/jbc.M100176200
87. Cuthbertson L, Kos V, Whitfield C. ABC transporters involved in export of cell surface glycoconjugates. Microbiol Mol Biol Rev 2010;74(3):341-62, doi:10.1128/mmbr.00009-10
88. Dawson RJ, Locher KP. Structure of the multidrug ABC transporter Sav1866 from Staphylococcus aureus in complex with AMP-PNP. FEBS Lett 2007;581(5):935-8, doi:10.1016/j.febslet.2007.01.073
89. Bi Y, Mann E, Whitfield C, et al. Architecture of a channel-forming O-antigen polysaccharide ABC transporter. Nature 2018;553(7688):361-365, doi:10.1038/nature25190
90. Chen L, Hou WT, Fan T, et al. Cryo-electron Microscopy Structure and Transport Mechanism of a Wall Teichoic Acid ABC Transporter. mBio 2020;11(2), doi:10.1128/mBio.02749-19
91. Li Y, Orlando BJ, Liao M. Structural basis of lipopolysaccharide extraction by the LptB(2)FGC complex. Nature 2019;567(7749):486-490, doi:10.1038/s41586-019-1025-6
92. Zeytuni N, Dickey SW, Hu J, et al. Structural insight into the Staphylococcus aureus ATP-driven exporter of virulent peptide toxins. Sci Adv 2020;6(40), doi:10.1126/sciadv.abb8219
93. MoBiTec GmbH G. Expression System for Lactococcus lactis. NIsin Controlled gene Expression system 2015;
94. Scheres SH. RELION: implementation of a Bayesian approach to cryo-EM structure determination. J Struct Biol 2012;180(3):519-30, doi:10.1016/j.jsb.2012.09.006
95. Punjani A, Rubinstein JL, Fleet DJ, et al. cryoSPARC: algorithms for rapid unsupervised cryo-EM structure determination. Nature Methods 2017;14(3):290-296, doi:10.1038/nmeth.4169

96. Zheng SQ, Palovcak E, Armache JP, et al. MotionCor2: anisotropic correction of beam-induced motion for improved cryo-electron microscopy. Nat Methods 2017;14(4):331-332, doi:10.1038/nmeth.4193
97. Rohou A, Grigorieff N. CTFFIND4: Fast and accurate defocus estimation from electron micrographs. Journal of Structural Biology 2015;192(2):216-221, doi:https://doi.org/10.1016/j.jsb.2015.08.008
98. Mi W, Li Y, Yoon SH, et al. Structural basis of MsbA-mediated lipopolysaccharide transport. Nature 2017;549(7671):233-237, doi:10.1038/nature23649
99. Caffalette CA, Zimmer J. Cryo-EM structure of the full-length WzmWzt ABC transporter required for lipid-linked O antigen transport. Proceedings of the National Academy of Sciences 2021;118(1):e2016144118, doi:doi:10.1073/pnas.2016144118
100. Hu W, Zheng H. Cryo-EM reveals unique structural features of the FhuCDB Escherichia coli ferrichrome importer. Communications Biology 2021;4(1):1383, doi:10.1038/s42003-021-02916-2
101. Gewering T, Januliene D, Ries AB, et al. Know your detergents: A case study on detergent background in negative stain electron microscopy. J Struct Biol 2018;203(3):242-246, doi:10.1016/j.jsb.2018.05.008
102. Denisov IG, Sligar SG. Nanodiscs for structural and functional studies of membrane proteins. Nature Structural & Molecular Biology 2016;23(6):481-486, doi:10.1038/nsmb.3195
103. Carlson ML, Young JW, Zhao Z, et al. The Peptidisc, a simple method for stabilizing membrane proteins in detergent-free solution. eLife 2018;7(e34085, doi:10.7554/eLife.34085
104. Frauenfeld J, Löving R, Armache J-P, et al. A saposin-lipoprotein nanoparticle system for membrane proteins. Nature Methods 2016;13(4):345-351, doi:10.1038/nmeth.3801
105. Pollock NL, Lee SC, Patel JH, et al. Structure and function of membrane proteins encapsulated in a polymer-bound lipid bilayer. Biochimica et Biophysica Acta (BBA) - Biomembranes 2018;1860(4):809-817, doi:https://doi.org/10.1016/j.bbamem.2017.08.012
106. Rigaud J-L, Lévy D. Reconstitution of Membrane Proteins into Liposomes. In: Methods in Enzymology. Academic Press: 2003; pp. 65-86.
107. Robinson PK. Enzymes: principles and biotechnological applications. Essays in Biochemistry 2015;59(1-41, doi:10.1042/bse0590001
108. Doige CA, Yu X, Sharom FJ. The effects of lipids and detergents on ATPase-active P-glycoprotein. Biochim Biophys Acta 1993;1146(1):65-72, doi:10.1016/0005-2736(93)90339-2
109. Kurauskas V, Hessel A, Ma P, et al. How Detergent Impacts Membrane Proteins: Atomic-Level Views of Mitochondrial Carriers in Dodecylphosphocholine. The Journal of Physical Chemistry Letters 2018;9(5):933-938, doi:10.1021/acs.jpclett.8b00269
110. Drulyte I, Johnson RM, Hesketh EL, et al. Approaches to altering particle distributions in cryo-electron microscopy sample preparation. Acta Crystallogr D Struct Biol 2018;74(Pt 6):560-571, doi:10.1107/s2059798318006496
111. Kim LY, Rice WJ, Eng ET, et al. Benchmarking cryo-EM Single Particle Analysis Workflow. Frontiers in Molecular Biosciences 2018;5(doi:10.3389/fmolb.2018.00050
112. Shaikh TR, Gao H, Baxter WT, et al. SPIDER image processing for single-particle reconstruction of biological macromolecules from electron micrographs. Nat Protoc 2008;3(12):1941-74, doi:10.1038/nprot.2008.156
113. Grigorieff N. Frealign: An Exploratory Tool for Single-Particle Cryo-EM. Methods Enzymol 2016;579(191-226, doi:10.1016/bs.mie.2016.04.013
114. Ludtke SJ, Baldwin PR, Chiu W. EMAN: semiautomated software for high-resolution single-particle reconstructions. J Struct Biol 1999;128(1):82-97, doi:10.1006/jsbi.1999.4174
115. Grant T, Rohou A, Grigorieff N. cisTEM, user-friendly software for single-particle image processing. eLife 2018;7(e35383, doi:10.7554/eLife.35383

116. Li X, Mooney P, Zheng S, et al. Electron counting and beam-induced motion correction enable near-atomic-resolution single-particle cryo-EM. Nature Methods 2013;10(6):584-590, doi:10.1038/nmeth.2472
117. Scheres SHW. Beam-induced motion correction for sub-megadalton cryo-EM particles. eLife 2014;3(e03665, doi:10.7554/eLife.03665
118. Jeong H-S, Park H-N, Kim J-G, et al. Critical importance of the correction of contrast transfer function fortransmission electron microscopy-mediated structural biology. Journal of Analytical Science and Technology 2013;4(1):14, doi:10.1186/2093-3371-4-14
119. Zhang X, Zhou ZH. Limiting factors in atomic resolution cryo electron microscopy: no simple tricks. J Struct Biol 2011;175(3):253-63, doi:10.1016/j.jsb.2011.05.004
120. Bepler T, Kelley K, Noble AJ, et al. Topaz-Denoise: general deep denoising models for cryoEM and cryoET. Nature Communications 2020;11(1):5208, doi:10.1038/s41467-020-18952-1
121. Marsh BP, Chada N, Sanganna Gari RR, et al. The Hessian Blob Algorithm: Precise Particle Detection in Atomic Force Microscopy Imagery. Scientific Reports 2018;8(1):978, doi:10.1038/s41598-018-19379-x
122. Jumper J, Evans R, Pritzel A, et al. Highly accurate protein structure prediction with AlphaFold. Nature 2021;596(7873):583-589, doi:10.1038/s41586-021-03819-2
123. Varadi M, Anyango S, Deshpande M, et al. AlphaFold Protein Structure Database: massively expanding the structural coverage of protein-sequence space with high-accuracy models. Nucleic Acids Research 2021;50(D1):D439-D444, doi:10.1093/nar/gkab1061
124. Lee J, Patel DS, Ståhle J, et al. CHARMM-GUI Membrane Builder for Complex Biological Membrane Simulations with Glycolipids and Lipoglycans. Journal of Chemical Theory and Computation 2019;15(1):775-786, doi:10.1021/acs.jctc.8b01066
125. Kampjut D, Steiner J, Sazanov LA. Cryo-EM grid optimization for membrane proteins. iScience 2021;24(3):102139, doi:https://doi.org/10.1016/j.isci.2021.102139
126. Narang D, Lento C, D JW. HDX-MS: An Analytical Tool to Capture Protein Motion in Action. Biomedicines 2020;8(7), doi:10.3390/biomedicines8070224
127. Masson GR, Burke JE, Ahn NG, et al. Recommendations for performing, interpreting and reporting hydrogen deuterium exchange mass spectrometry (HDX-MS) experiments. Nature Methods 2019;16(7):595-602, doi:10.1038/s41592-019-0459-y
128. Cryar A, Groves K, Quaglia M. Online Hydrogen-Deuterium Exchange Traveling Wave Ion Mobility Mass Spectrometry (HDX-IM-MS): a Systematic Evaluation. J Am Soc Mass Spectrom 2017;28(6):1192-1202, doi:10.1007/s13361-017-1633-z
129. Gulezian E, Crivello C, Bednenko J, et al. Membrane protein production and formulation for drug discovery. Trends in Pharmacological Sciences 2021;42(8):657-674, doi:https://doi.org/10.1016/j.tips.2021.05.006
130. Sadaf A, Ramos M, Mortensen JS, et al. Conformationally Restricted Monosaccharide-Cored Glycoside Amphiphiles: The Effect of Detergent Headgroup Variation on Membrane Protein Stability. ACS Chem Biol 2019;14(8):1717-1726, doi:10.1021/acschembio.9b00166
131. Sigworth FJ. Principles of cryo-EM single-particle image processing. Microscopy 2015;65(1):57-67, doi:10.1093/jmicro/dfv370
132. Langlois R, Pallesen J, Frank J. Reference-free particle selection enhanced with semi-supervised machine learning for cryo-electron microscopy. J Struct Biol 2011;175(3):353-61, doi:10.1016/j.jsb.2011.06.004